



A new Dead Sea pollen record reveals the last glacial paleoenvironment of the southern Levant



Andrea Miebach ^{a,*}, Sophie Stolzenberger ^b, Lisa Wacker ^c, Andreas Hense ^c, Thomas Litt ^a

^a Institute of Geosciences and Meteorology, Section Palaeontology, University of Bonn, Nussallee 8, 53115, Bonn, Germany

^b Institute of Geodesy and Geoinformation, University of Bonn, Nussallee 17, 53115, Bonn, Germany

^c Institute of Geosciences and Meteorology, Section Meteorology, University of Bonn, Auf dem Hügel 20, 53121, Bonn, Germany

ARTICLE INFO

Article history:

Received 9 October 2018

Received in revised form

26 April 2019

Accepted 29 April 2019

Available online 14 May 2019

Keywords:

Eastern Mediterranean

Vegetation dynamics

Fire history

Paleoclimate

Anatomically modern humans

ICDP Dead Sea deep drilling project

Lake Lisan

Late Pleistocene

Biome modeling

Micro-charcoal

ABSTRACT

The southern Levant is a key region for studying vegetation developments in relation to climate dynamics and hominin migration processes in the past due to the sensitivity of the vegetation to climate variations and the long history of different anthropogenic occupation phases. However, paleoenvironmental conditions in the southern Levant during the Late Pleistocene were still insufficiently understood. Therefore, we investigated the vegetation and fire history of the Dead Sea region during the last glacial period. We present a new palynological study conducted on sediments of Lake Lisan, the last glacial precursor of the Dead Sea. The sediments were recovered from the center of the modern Dead Sea within an ICDP campaign. The palynological results suggest that Irano-Turanian steppe and Saharo-Arabian desert vegetation prevailed in the Dead Sea region during the investigated period (ca. 88,000–14,000 years BP). Nevertheless, Mediterranean woodland elements significantly contributed to the vegetation composition, suggesting moderate amounts of available water for plants. The early last glacial was characterized by dynamic climate conditions with pronounced dry phases and high but unstable fire activity. Anatomically modern humans entered the southern Levant during a climatically stable phase (late MIS 4–MIS 3) with diverse habitats, constant moisture availability, and low fire activity. MIS 2 was the coldest phase of the investigated timeframe, causing changes in woodland composition and a widespread occurrence of steppe. We used a biome modeling approach to assess regional vegetation patterns under changing climate conditions and to evaluate different climate scenarios for the last glacial Levant. The study provides new insights into the environmental responses of the Dead Sea region to climate variations through time. It contributes towards our understanding of the paleoenvironmental conditions in the southern Levant, which functioned as an important corridor for human migration processes.

© 2019 The Authors. Published by Elsevier Ltd. This is an open access article under the CC BY license (<http://creativecommons.org/licenses/by/4.0/>).

1. Introduction

The study of the paleoclimate and its influences on environments is essential not only to understand current and future climate changes (Masson-Delmotte et al., 2013) but also to reconstruct the history of mankind. The Levant in the southeastern Mediterranean region is a possible meeting point of anatomically modern humans (AMH) and Neanderthals, where gene flow between the two hominins may have occurred (Kuhlwilm et al., 2016). The Levantine fossil record provides evidence for the first migration

of AMH out of Africa (Hershkovitz et al., 2018) and for later hominin migration processes towards Eurasia (Mellars, 2011). A renewed migration of AMH out of Africa, probably leading to the occupation of Europe, took place during the last glacial. Earliest fossil evidence dated to ca. 55 ka BP (kilo years before present; all radiocarbon dates in this paper have been calibrated) originates from Manot Cave, Israel (Hershkovitz et al., 2015). In addition, the extinction of Neanderthals occurred during the last glacial, namely between 45 and 30 ka BP, leading to ongoing discussions about the causes (Shea, 2008). Among others, climatic causes have been postulated for AMH migration and Neanderthal extinction processes (e.g., Shea, 2008; Müller et al., 2011).

However, there are ongoing discussions on the hydroclimatic conditions in the southern Levant during the last glacial. While the

* Corresponding author.

E-mail address: a.miebach@uni-bonn.de (A. Miebach).

majority of climate records from the Eastern Mediterranean agree on cold and arid conditions during the last glacial (e.g., Fleitmann et al., 2009; Langgut et al., 2011; Müller et al., 2011; Pickarski et al., 2015), most studies from the Dead Sea region suggest more humid conditions compared to today. Indications for an increased glacial wetness were provided by various studies dealing, for instance, with lake-level reconstructions, geochemical compositions of sediments, and speleothem activities. Lake-level reconstructions of Lake Lisan, the precursor of the Dead Sea, indicate major lake-level high stands during the last glacial of up to ca. 240 m above typical Holocene levels (e.g., Bartov et al., 2002; Torfstein et al., 2013b). During the highest stands, Lake Lisan even merged with the Sea of Galilee (Bartov et al., 2003; Hazan et al., 2005; Torfstein et al., 2013b), being separated today by more than 100 km. The sediments that deposited during the occurrence of Lake Lisan are mainly comprised of aragonite-detritus laminae (e.g., Begin et al., 1974; Katz et al., 1977; Machlus et al., 2000). Aragonite formation requires an increased input of freshwater to the lake to provide bicarbonate to the Ca-chloride brine (Stein et al., 1997; Barkan et al., 2001). Therefore, the high lake levels and aragonite deposition might indicate increased precipitation rates during the last glacial (Stein et al., 1997; Torfstein et al., 2013b). Increased glacial wetness is also suggested by the deposition of speleothems in areas that were too dry for speleothem growth during the Holocene (Vaks et al., 2003, 2006; Bar-Matthews et al., 2017).

Despite its outstanding role in terms of archeology and paleoclimate, little was known about the paleovegetational conditions in the southern Levant during the last glacial. The study of fossil pollen and other palynomorphs contained in sediments enables the reconstruction of past environments, particularly the paleo-vegetation and paleoclimate (Faegri and Iversen, 1989). However, a detailed palynological study based on an independent chronology was still missing for the last glacial Dead Sea region.

Previous palynological studies from the Levant were either based on marine or terrestrial sediments. Marine studies were conducted in the Levantine Basin and suggest cold and dry glacial conditions (Cheddadi and Rossignol-Strick, 1995; Langgut et al., 2011). However, the pollen assemblages reflect a huge pollen source area given the basin size and were influenced by African vegetation due to the Nile outflow (Langgut, 2018). A terrestrial pollen record encompassing the whole last glacial was obtained from Yammouneh Basin, Lebanon (Gasse et al., 2011, 2015). This study also indicates warm and wet interglacials and cold and dry glacials. However, given the high altitude of the Yammouneh Basin, the vegetation might have been influenced by water deficiencies due to water storage as ice or frozen soils (Develle et al., 2011). The same orographic climate effect might have affected the Birkat Ram area on the Golan Heights, where palynological results for the last 30 ka suggest a similar vegetation pattern (Schiebel, 2013). Strikingly, a last glacial sequence from the Sea of Galilee, located in the Jordan Valley below sea level, also indicates less water availability for plants compared to the Holocene (Miebach et al., 2017). Pollen records from the Hula Basin, northern Israel, might also encompass large parts or even the whole last glacial period (e.g., Horowitz, 1979; Weinstein-Evron, 1983). However, problems with radiocarbon (^{14}C) dating (e.g., Meadows, 2005; van Zeist et al., 2009) and Uranium–Thorium (U–Th) dating (Weinstein-Evron et al., 2001) of sediment cores from Hula Basin make a convincing correlation to other records difficult. Major chronological uncertainties also occur in a sediment core from the Ghab Valley, northwestern Syria. The pollen sequence suggested the spread of Mediterranean forests during marine isotope stages (MIS) 3 and 2 (Niklewski and van Zeist, 1970). However, Rossignol-Strick (1995) revised the chronology to a late glacial and Holocene age. Horowitz (1992) presented a vegetation model for the Dead Sea region during the Late

Quaternary based on several low-resolution pollen sequences. The correlation to climate records was based on few age determinations and the following hypothesis: during times corresponding to even numbered MIS, woodland vegetation predominated (e.g., MIS 4 and 2), while periods corresponding to odd numbered MIS were characterized by the dominance of steppe vegetation (e.g., MIS 3 and 1) and/or desert vegetation (e.g., MIS 5 and 1). Therefore, further knowledge is required about the vegetation history of the Levantine lowlands based on a terrestrial high-resolution pollen record with a robust chronology.

The study of microscopic charcoal can provide valuable insights into the history of fire activity and the relationship between the paleovegetation, anthropogenic activities, and fire regimes (Whitlock and Larsen, 2001). However, almost none of the last glacial palynological studies from the Levant investigated micro-charcoal in addition to pollen. Exceptions are studies from the Ghab Valley (Yasuda et al., 2000) and the Hula Basin (Turner et al., 2010) dating to the late glacial and Holocene. However, large uncertainties in the radiocarbon chronologies of the sediment cores from the Ghab Valley and the Hula Basin (e.g., Meadows, 2005; van Zeist et al., 2009) make the timing of events and the correlation to other records speculative. Still, these records provide comparisons between changes in fire activity and vegetation because charcoal and pollen originated from the same sediment sequences. The fire history during earlier times of the last glacial and particularly at the Dead Sea remained unknown.

Here, we present a new palynological study conducted on sediments of the last glacial Lake Lisan (Lisan Formation). The investigated sediments were recovered in the framework of the International Continental Scientific Drilling Program (ICDP) from the central Dead Sea (Stein et al., 2011a, b) and have an independent chronology based on ^{14}C and U–Th dating (Neugebauer et al., 2014; Torfstein et al., 2015; Kitagawa et al., 2017). The palynological study provides new and detailed insights into the last glacial vegetation and fire history of the southern Levant in relation to climate changes. We test previous hypotheses on the paleovegetation in the Dead Sea region, namely the coincidence of woodland expansion and retraction with marine isotope stages (Horowitz, 1992). We evaluate climate scenarios for the last glacial Levant regarding their influence on the biome distribution using a biome-climate transfer function and the accordance with the new palynological dataset. In addition, we draw conclusions about the paleoenvironmental setting for occupation phases of AMH and Neanderthals.

2. Study area

2.1. Dead Sea

The Dead Sea is situated in the southern Levant bordering Israel, Jordan, and the Palestinian Territory West Bank (Fig. 1). It is a terminal lake and is primarily fed by the perennial Jordan River but also by groundwater and several streams, which are mainly ephemeral, i.e., they experience occasional flashfloods. The total drainage area comprises 42,200 km² (Greenbaum et al., 2006). The Dead Sea occupies the lowest continental depression on Earth (currently ca. 430 m below mean sea level (m bmsl)). With a surface area of about 760 km² (76 km in N–S direction, up to 17 km in W–E direction), it is the largest lake in the region (Litt et al., 2012). A sill separates a northern deep basin with a water depth of about 300 m from a shallower southern basin. While the water depth of the northern basin has been steadily declining during the last decades due to human impact, the southern basin is nowadays occupied by evaporation ponds (Greenbaum et al., 2006). The Dead Sea is a hypersaline water body with a salinity of ca. 27.5% (ca. 340 g/l), i.e., the salinity is multiple times higher compared to seawater (Gavrieli



Fig. 1. Topography of the southern Levant with Dead Sea drainage and maximum extent of Lake Lisan after Greenbaum et al. (2006).

and Stein, 2006).

The Dead Sea is located at the Dead Sea Transform, a tectonic boundary between the Sinai and Arabian plates. The Dead Sea Basin is the largest and oldest of several pull-apart basins, which originated along the transform during the plate motion process (Garfunkel, 2014). Since its formation in the early Miocene, the Dead Sea Basin subsided continuously and acted as a major sediment trap (Garfunkel, 1997). During the late Neogene, the valley

was filled with water coming from the Mediterranean Sea and forming the marine Sedom Lagoon (Stein, 2014). After the disconnection of the Sedom Lagoon from the Mediterranean Sea, the Dead Sea Basin was occupied by a series of lakes. One of them was Lake Lisan, which occurred during the last glacial. While chronostratigraphic analyses at the shore indicate an age of ca. 70 to 15 ka BP for the duration of Lake Lisan (e.g., Torfstein et al., 2013a), the new ICDP core drilled at the deepest part of the Dead Sea suggest that the

transition to Lake Lisan occurred ca. 15–20 ka earlier (Neugebauer et al., 2016).

2.2. Climate and vegetation

The southern Levant is a transition zone of different climate regimes (Fig. 2). The northern part is characterized by a Mediterranean climate with hot, dry summers and mild, wet winters. The precipitation is mainly brought by Mediterranean mid-latitude cyclones, e.g. Cyprus Lows (Enzel et al., 2003; Goldreich, 2003). The southern part is occupied by a dry, subtropical desert (Kushnir et al., 2017). Here, precipitation arrives mainly as flash floods by the tropical Active Red Sea Trough (Dayan and Morin, 2006). While precipitation rates generally decrease towards the south and with lower elevations, temperatures generally decrease towards the north and with higher elevations. Seasonality increases towards the east (Goldreich, 2003). The Dead Sea itself lies in a hyperarid area with 50–100 mm mean annual precipitation (Greenbaum et al., 2006).

The natural vegetation of the southern Levant is primarily shaped by the precipitation distribution but also by temperatures and soils (Fig. 2; Zohary, 1962, 1982; Danin and Plitmann, 1987; Danin, 1992). The northern part is characterized by the Mediterranean biome with arboreal climax communities. Mediterranean woodland reaches southward to the Judean Mountains and along the upper slopes of the Rift Valley east of the Dead Sea. The area receives 350–1200 mm mean annual precipitation (Zohary, 1962). Common trees are deciduous *Quercus* (mostly *Q. ithaburensis* and

Q. boissieri; *Q. libani* at high elevations), evergreen *Quercus* (*Q. calliprinos*), *Pistacia* spp., *Ziziphus* spp., *Rhamnus* spp., *Ceratonia siliqua*, *Phillyrea latifolia*, *Styrax officinalis*, *Arbutus andrachne*, and several Rosaceae species. They are accompanied by conifers such as *Pinus halepensis* and *Juniperus* spp. (Baruch, 1986 and references therein; Danin, 1992). Irano-Turanian steppe occupies areas with ca. 100–350 mm mean annual precipitation. It is characterized by herb and dwarf-shrub communities dominated by *Artemisia herba-alba*. Saharo-Arabian desert vegetation occurs in the southern part, where the mean annual precipitation falls below 100 mm. It is a vegetation type with sparse plant cover and low diversity. Important representatives of the Saharo-Arabian vegetation are Amaranthaceae. Sudanian vegetation occupies tropical oases of the Jordan Valley. Mainly trees and shrubs such as *Maerua crassifolia*, *Acacia tortilis*, *Balanites aegyptiaca*, and *Ziziphus spina-christi* compose this vegetation type (Zohary, 1962).

3. Material and methods

3.1. Drilling campaign and stratigraphy

The Dead Sea Deep Drilling Project (DSDDP) under the auspices of the ICDP was intended to gain the first long, continuous, and high-resolution sediment sequence from the Dead Sea. The drilling campaign took place in 2010/2011 (Stein et al., 2011a, b). We analyzed sediment samples from the deepest borehole (core 5017-1-A, site 5017-1, N 31°30'28.98", E 35°28'15.60") with a total drilled length of 455.34 m. It is located at the center of the northern basin

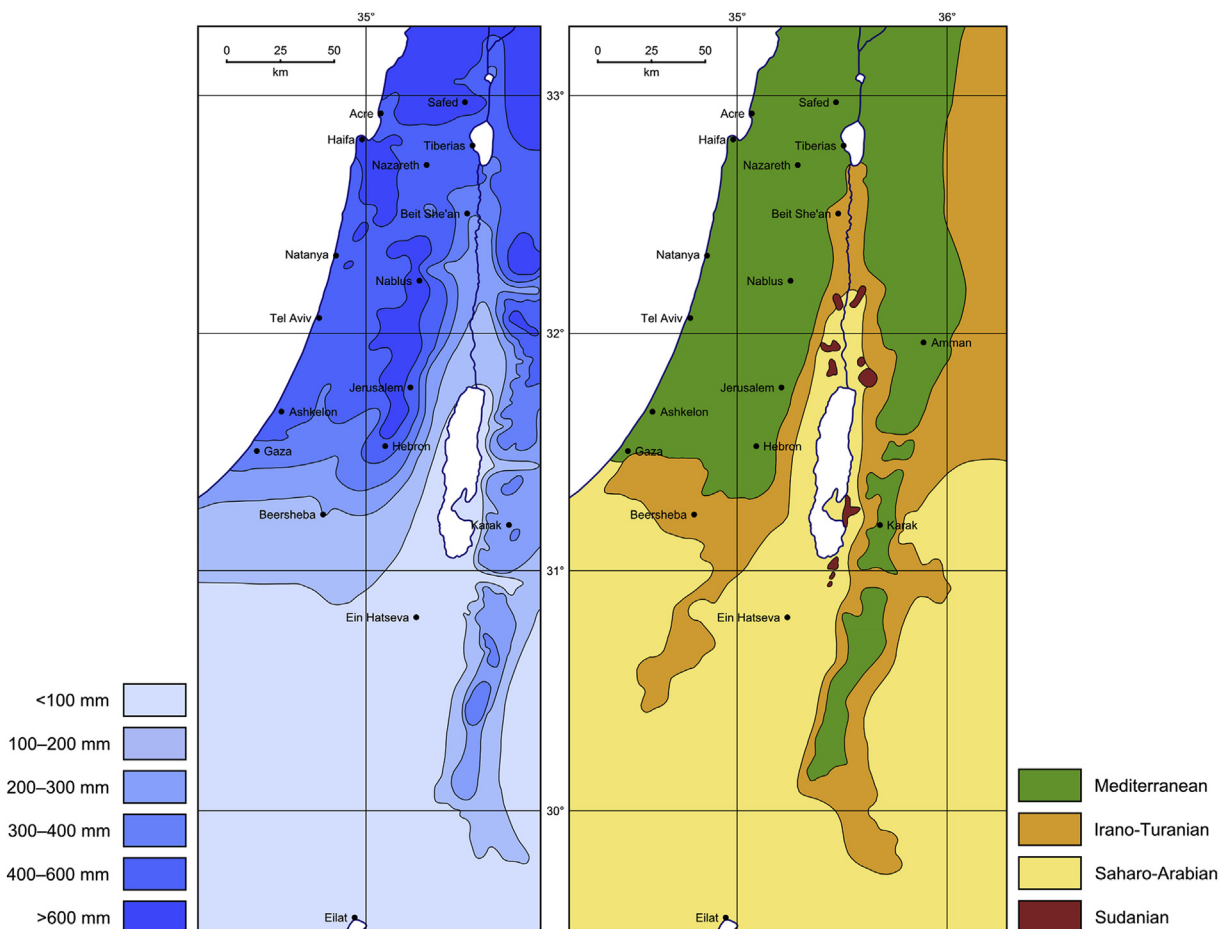


Fig. 2. Mean annual precipitation and plant-geographical territories of the southern Levant after Zohary (1962).

(Fig. 1). In this study, the sediment depth of the analyzed samples encompasses 199.07–92.35 m. The investigated interval belongs to the Lisan Formation (Neugebauer et al., 2014, 2016). 76% of the Lisan Formation of the 5017-1-A core are mass transport deposits (MTDs), showing disturbed, slumped, and homogenous sediment sections. The remaining sediments are composed of laminated alternating aragonite and detritus (aad facies) with some gypsum laminae (Kagan et al., 2018). We only sampled the latter facies, resulting in sampling gaps of different length.

3.2. Chronology

The current chronology of the investigated sediment sequence is based on a linear interpolation of published ^{14}C and U–Th dates (Table 1). Twelve ^{14}C dates were conducted from terrestrial plant remains of core 5017-1-A (Neugebauer et al., 2014; Kitagawa et al., 2017). We calibrated the ^{14}C dates using the calibration dataset IntCal13 (Reimer et al., 2013) within the software OxCal 4.2 (Ramsey, 2009). U–Th dating was performed on four samples of primary aragonite from core 5017-1-A (for more details see Torfstein et al., 2015). In addition, Torfstein et al. (2015) correlated a massive gypsum deposit in the 5017-1-A core to U–Th dated counterparts in exposed margins of the Dead Sea Basin (Torfstein et al., 2013a). To account for the high number of MTDs in the Lisan Formation, we constructed an event-free age-depth model following Kagan et al. (2018). MTDs larger than 50 cm (Fig. 5) were excluded from the model. Debris (homogenites, turbidites, and breccias) were completely removed, whereas slumps were considered to include some original laminae. Thus, only 2/3 of the slump thickness was excluded. According to the age-depth model, the investigated sediment section of this study encompasses ca. 88–14 ka BP.

3.3. Palynological analyses

Pollen preparation of 203 sediment samples with a sample volume of mostly 4–6 cm^3 was processed following a standard protocol described by Faegri and Iversen (1989). The chemical treatment included 10% hydrochloric acid (HCl) for 10 min, 40% hydrofluoric acid (HF) for 48 h, 10% hot HCl for 10 min, glacial acetic acid ($\text{C}_2\text{H}_4\text{O}_2$), hot acetolysis with 1 part concentrated sulfuric acid (H_2SO_4) and 9 parts concentrated acetic anhydride ($\text{C}_4\text{H}_6\text{O}_3$) for a maximum of 3 min, and $\text{C}_2\text{H}_4\text{O}_2$. Sieving and ultrasonic sieving

were carried out to remove particles coarser than 200 μm and particles finer than 10 μm , respectively. *Lycopodium* tablets with a known number of spores were added to each sample to calculate pollen, non-pollen palynomorph, and micro-charcoal concentrations (Stockmarr, 1971). Samples were preserved in glycerol and were stained with safranin.

Palynomorphs were identified with a Zeiss Axio Lab.A1 light microscope with the help of palynomorph atlases and keys (Reille, 1995, 1998, 1999; Beug, 2004) as well as the pollen reference collection of the Institute of Geosciences and Meteorology, University of Bonn. At least 500 terrestrial pollen grains were counted in each sample. Obligate aquatic plants were not included in the terrestrial pollen sum to exclude local taxa growing in the lake (Moore et al., 1991). Furthermore, destroyed and unknown pollen were excluded from the terrestrial pollen sum, which was used to calculate percentages of the pollen assemblage. *Quercus* pollen was grouped into two morphotypes. Evergreen *Quercus* pollen was separated from deciduous *Quercus* pollen according to the morphological features of the evergreen *Q. ilex* type (Beug, 2004). The pollen types were named after evergreen *Q. calliprinos* and deciduous *Q. ithaburensis*, respectively – today's most common species in the region – following the nomenclature rules by Birks (1973). Some pollen types were grouped to higher taxonomic levels in the summary pollen diagrams. Likewise, *Alnus*, *Fraxinus excelsior* type, *Platanus orientalis*, *Salix*, *Tamarix*, *Ulmus/Zelkova*, and *Vitis* were grouped to riverine trees and shrubs following van Zeist et al. (2009). Pollen count ratios of *Artemisia* to Amaranthaceae (A/A) and *Quercus ithaburensis* type to Amaranthaceae (Q/A) were calculated to evaluate their use as climate indicators (El-Moslimany, 1990; Zhao et al., 2012). Charcoal particles were divided into two size fractions with diameters of 25–100 μm and 100–200 μm . If the size fraction is not stated hereafter, the sum of both fractions is given.

A stratigraphically constrained cluster analysis using a square root transformation was performed by CONISS (Grimm, 1987) to aid pollen zonation. All taxa with more than 1% of the terrestrial pollen sum and the sum of trees and shrubs were used for the analysis. Pollen diagrams were prepared with the software Tilia, Version 2.0.41 (© 1991–2015 Eric C. Grimm).

3.4. Biome modeling

The (Bayesian) biome model (Schölzel, 2006; Litt et al., 2012;

Table 1
Radiocarbon (^{14}C) dates of terrestrial plant remains and Uranium–Thorium (U–Th) dates of Dead Sea core 5017-1-A with sediment depths. The median of calibrated ages is given for ^{14}C dates. AMS: accelerator mass spectroscopy.

Depth (m)	Uncalibrated radiocarbon age (a BP)	Calendar age	Technique	Source
92.06	12,240 ± 57	14,145 a cal BP	AMS ^{14}C	Neugebauer et al. (2014)
98.51	13,450 ± 60	16,184 a cal BP	AMS ^{14}C	Kitagawa et al. (2017)
102.49	13,865 ± 40	16,794 a cal BP	AMS ^{14}C	Kitagawa et al. (2017)
102.8	14,130 ± 65	17,199 a cal BP	AMS ^{14}C	Kitagawa et al. (2017)
104.8	15,085 ± 65	18,335 a cal BP	AMS ^{14}C	Kitagawa et al. (2017)
106	16,660 ± 75	20,102 a cal BP	AMS ^{14}C	Kitagawa et al. (2017)
108.51	17,360 ± 75	20,942 a cal BP	AMS ^{14}C	Neugebauer et al. (2014)
113.8	25,020 ± 160	29,061 a cal BP	AMS ^{14}C	Kitagawa et al. (2017)
115.37	26,046 ± 165	30,340 a cal BP	AMS ^{14}C	Neugebauer et al. (2014)
131.62	31,710 ± 310	35,606 a cal BP	AMS ^{14}C	Kitagawa et al. (2017)
139.27		41,799 ± 935 a BP	U–Th	Torfstein et al. (2015)
139.33	38,200 ± 390	42,364 a cal BP	AMS ^{14}C	Kitagawa et al. (2017)
139.60	40,250 ± 835	43,946 a cal BP	AMS ^{14}C	Neugebauer et al. (2014)
144.5		46,000 ± 1700 a BP	Correlated U–Th ^a	Torfstein et al. (2015, 2013a)
174.52		70,513 ± 4926 a BP	U–Th	Torfstein et al. (2015)
193.58		85,557 ± 8176 a BP	U–Th	Torfstein et al. (2015)
220.03		102,091 ± 8625 a BP	U–Th	Chen and Litt (2018) modified after Torfstein et al. (2015)

^a A massive gypsum unit of core 5017-1-A was correlated to U–Th dated on-shore counterparts.

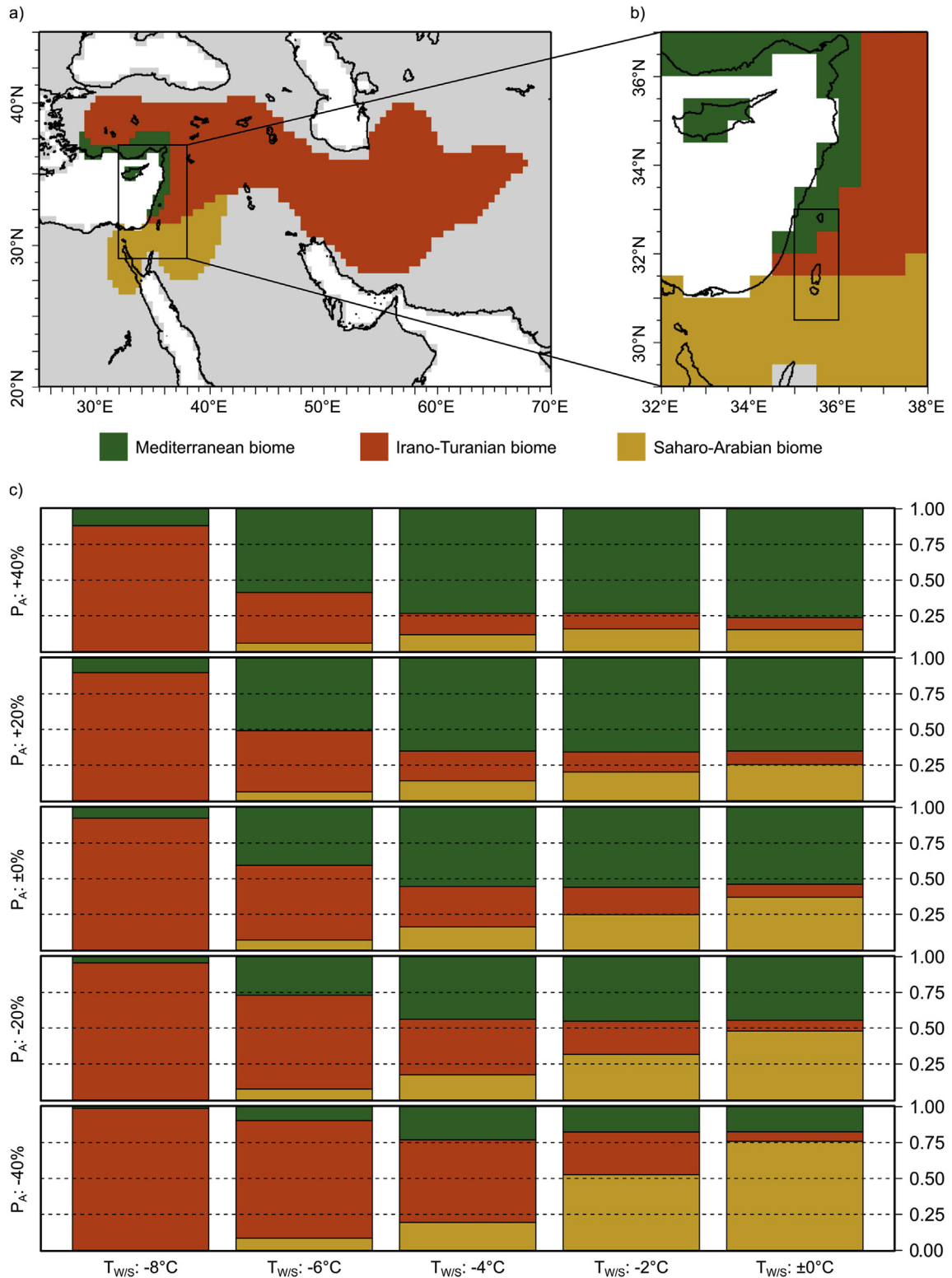


Fig. 3. a) Original biome distribution (Meusel et al., 1965; Thoma, 2017) used for biome modeling, b) original biome distribution in the Levant, c) modeled probability for the occurrence of biomes in the surrounding of Lake Lisan under changed climate parameters (the analyzed area is marked by the box in b). P_A = annual precipitation sum, T_{WS} = mean summer and winter temperature.

Ohlwein and Wahl, 2012) is generally used for probabilistic reconstructions of past climate states given a biome distribution. It includes the probability for the occurrence of each biome given the corresponding pollen spectra, the biome-climate transfer function

(also called likelihood function), and a prior probability distribution. In this study, spatial variations of the biomes in the Levant – the Mediterranean, Irano-Turanian, and Saharo-Arabian biome – were modeled using climate information. Therefore, we estimated

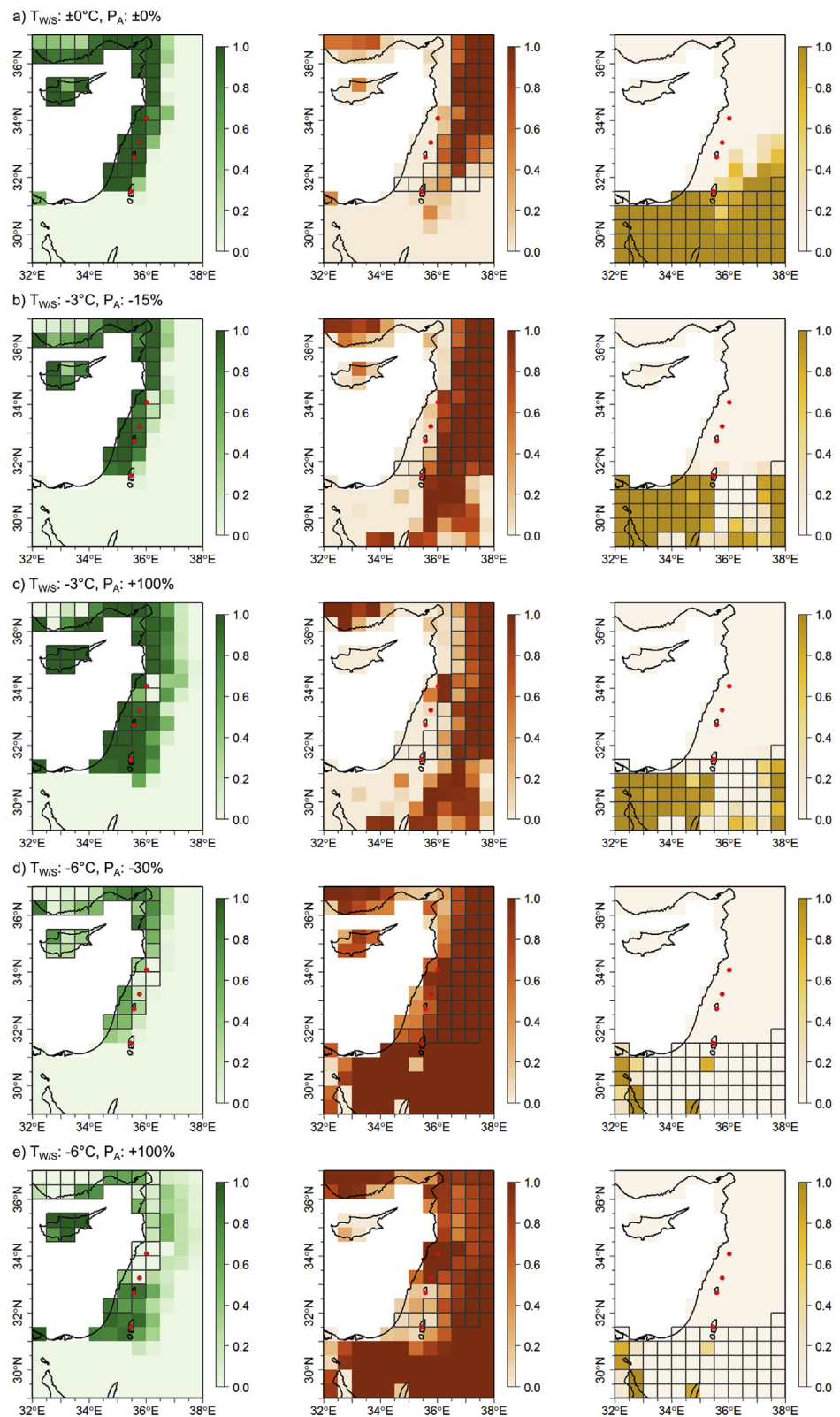


Fig. 4. Modeled biome distribution with probabilities for each biome (left: Mediterranean biome, central: Irano-Turanian biome, right: Saharo-Arabian biome) for different climate scenarios: a) unchanged climate conditions, b–e) changed climate parameters according to climate scenarios in the literature (see text). P_A = annual precipitation sum. $T_{W/S}$ = mean summer and winter temperature. Red dots indicate the sites Yammouneh, Birkat Ram, Sea of Galilee, and Dead Sea (from north to south). Grey grids indicate the original biome distribution of the respective biome. (For interpretation of the references to colour in this figure legend, the reader is referred to the Web version of this article.)

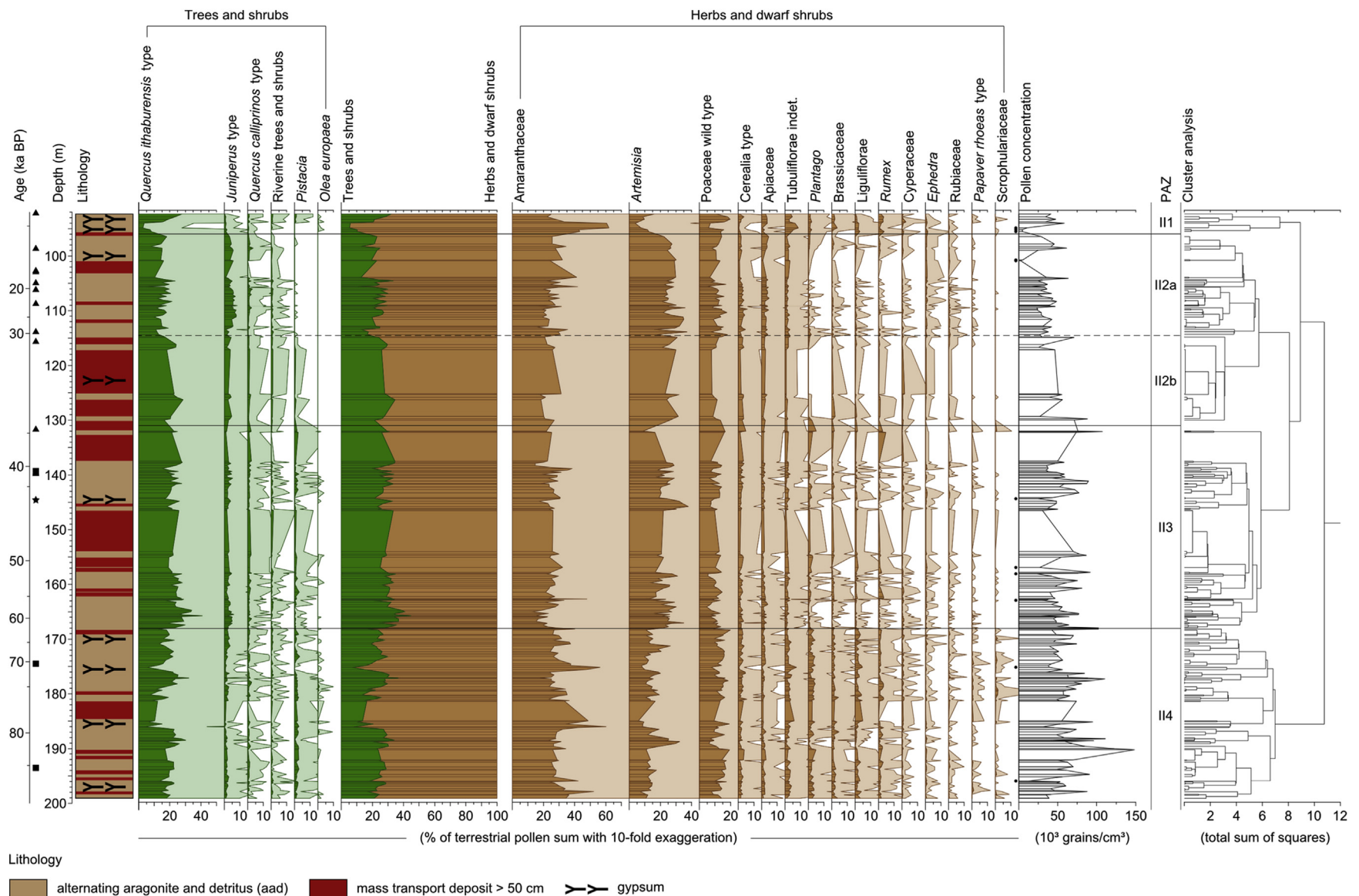


Fig. 5. Pollen diagram of Dead Sea core 5017-1-A plotted against depth with most abundant taxa, pollen concentrations with dots indicating gypsum in pollen sample, cluster analysis, and PAZs (pollen assemblage zones). The lithology is modified after Kagan et al. (2018) with gypsum deposits after Neugebauer et al. (2014). The chronology is based on a linear interpolation of calibrated radiocarbon dates (triangles), Uranium–Thorium dates (squares), and a correlated Uranium–Thorium date (star).

only the biome-climate transfer function in the biome model – the probability for the occurrence of a biome given a certain climate state. This probability was determined by using a quadratic discriminant analysis (QDA), where the probability for each biome is dependent on the other two biomes and where the probabilities are normalized to one.

We used the CRU version 4.01 dataset comprising monthly terrestrial climate parameters for the period from 1901 to 2016. This global dataset was created by interpolating quality checked station data on a regular $0.5^\circ \times 0.5^\circ$ latitude-longitude grid (Harris et al., 2014). We used three climate parameters, namely annual precipitation, winter temperature (average December, January, February values), and summer temperature (average June, July, August values). The recent biome distribution is based on vegetation maps by Meusel et al. (1965) that were digitized on the same grid (Fig. 3a and b; Schölzel et al., 2002; Litt et al., 2012; Thoma, 2017).

Biome modeling was performed using the freely available R software (R Core Team, 2016). Further details of the model, including the mathematical description, were given by Ohlwein and Wahl (2012) and Litt et al. (2012).

4. Results and discussion

4.1. Biome modeling

We performed biome modeling to explore the spatial implications of Levantine biomes in response to climate fluctuations. A series of plotted scenarios (Fig. 3c) draw clues about the climatic sensitivity of biomes in the surrounding of Lake Lisan (Fig. 3b). The model reveals major biome shifts in response to precipitation and temperature changes: I) The Mediterranean biome spreads with increasing precipitation, but only a temperature reduction of more than 4°C causes a decline of the Mediterranean biome; II) Decreasing temperatures trigger a spread of the Irano-Turanian biome, while precipitation changes do not necessarily alter the Irano-Turanian biome distribution; III) The Saharo-Arabian biome shrinks under colder conditions and with increasing precipitation.

The model enables us to explore the spatial distribution of biomes under various climate scenarios for the last glacial period though does not account for changing boundary conditions such as atmospheric CO₂ and insolation variations. Given the existing pollen data of the region, those scenarios can be evaluated. Several studies have estimated the glacial temperature in the southern Levant based on proxy data or climate models. For MIS 3, those temperature estimations range between a reduction of ca. $2\text{--}5^\circ\text{C}$ with a mean of ca. 3°C ($\sim 2^\circ\text{C}$) (Stockhecke et al., 2016), 3°C (Affek et al., 2008), Ø 3.5°C (McGarry et al., 2004), Ø 4.9°C (Almogi-Labin et al., 2009)). For MIS 2, temperature reduction estimations range between ca. $3\text{--}8^\circ\text{C}$ with a mean of ca. 6°C (-3°C) (Zaarur et al., 2016), $\sim 4^\circ\text{C}$ (Stockhecke et al., 2016), Ø 6.5°C (Affek et al., 2008), Ø 7.6°C (McGarry et al., 2004), Ø 8.2°C (Almogi-Labin et al., 2009)). Despite ongoing discussions on glacial precipitation in the southern Levant (e.g., Torfstein et al., 2013b), few studies are available that quantify the amount of precipitation for the last glacial. Enzel et al. (2008) and Vaks et al. (2006) suggest a doubling of annual precipitation based on rates of aragonite deposition in Lake Lisan and speleothem growth in the northern Negev. Rohling (2013) and Barkan et al. (2001) even assume a 5-fold and 6-fold precipitation rate compared to today, respectively. In contrast, Stockhecke et al. (2016) suggest a reduction of annual precipitation for the last glacial Levant, i.e., ca. 15% during MIS 3 and ca. 30% during MIS 2 (Stockhecke et al., 2016: Fig. 12).

In addition, various aspects of seasonality changes were discussed for the last glacial climate. Such are, for example, an

increased precipitation seasonality (Prentice et al., 1992), a decreased precipitation seasonality (Orland et al., 2012), an increased frequency of floods (Ben Dor et al., 2018), and a seasonal moisture deficit due to increased snowfall (Robinson et al., 2006). While we assess total precipitation changes in the biome model, the current biome model does not account for seasonality changes. Still, we discuss the influence of glacial seasonality changes on plants in section 4.3.4.

The modeled biome distribution given the different climate scenarios (Fig. 4b–e) illustrates the variability of recent hypotheses in the literature. All vegetation patterns differ considerably from today's modeled biome distribution with unchanged climate parameters (Fig. 4a). The reduction of temperature particularly favors the Irano-Turanian biome, which replaces the Saharo-Arabian biome over a wide area. In some areas such as the Yammouneh Basin, the temperature decline triggers a limitation of the Mediterranean biome due to orographic effects such as frozen soils and snowfall (cf. Develle et al., 2011). Precipitation changes have major impacts on the Mediterranean biome. While an increased precipitation facilitates the spread of the Mediterranean biome, particularly southeast of the Dead Sea, precipitation declines reduce the probability of the Mediterranean biome occurrence.

The biome model outputs are discussed regarding their coincidence with regional pollen data in sections 4.3.3 and 4.3.4.

4.2. Pollen zonation

The results of the palynological investigation are summarized in Table 2 and Figs. 5 and 6. Five pollen assemblage zones (PAZs) were defined according to the cluster analysis (Fig. 5). The Roman numeral II follows the hierarchical classification of pollen assemblage superzones after Tzedakis (1994) for a better overview of future synthesis pollen records from the whole Dead Sea profile 5017-1 (see also Chen and Litt, 2018).

4.3. Vegetation, fire, and climate history

4.3.1. General remarks and interpretations

The vegetation in the Dead Sea region was generally dominated by open vegetation during the last glacial period (ca. 88–14 ka BP; Figs. 5 and 6). Large pollen amounts of Amaranthaceae (amaranth family including the former goosefoot family Chenopodiaceae), *Artemisia*, and Poaceae (grasses) indicate the widespread occurrence of herb and dwarf-shrub communities. Amaranthaceae are the main representatives of the Saharo-Arabian desert biome, which nowadays receives very low annual precipitation values of 100 mm or less (Zohary, 1962; Litt et al., 2012). The plant family contains many drought-adapted and salinity-tolerant species (Rossignol-Strick, 1995; van Zeist et al., 2009). *Artemisia* is the dominant plant of today's Irano-Turanian steppe biome (Zohary, 1962) and tolerates aridity though less extreme than Amaranthaceae (Rossignol-Strick, 1995). *Artemisia* is adapted to somewhat higher precipitation rates of ca. 100–350 mm (Zohary, 1962). Modern studies showed that *Artemisia* pollen increases and Amaranthaceae pollen decreases with decreasing aridity. Therefore, A/A ratios can be used as a moisture indicator, particularly in primary non-forested areas (El-Moslimany, 1990; Zhao et al., 2012). The expansion of Irano-Turanian steppe and suppression of Saharo-Arabian desert under reduced temperatures, as shown by the biome model (Figs. 3 and 4), implies that increased A/A ratios can also be indicative of reduced temperatures. Poaceae are also associated with the Irano-Turanian steppe biome (Litt et al., 2012), particularly humid steppes (van Zeist and Bottema, 2009). Yet, its various species also admix into a range of vegetation types (Danin, 1992, 1999). Poaceae comprise of a wild pollen type and a Cerealia

Table 2

Pollen assemblage zones (PAZs) with depths, ages, mean spatial and temporal resolution of samples, main components of pollen assemblages (arboreal pollen (AP) and non-arbooreal pollen (NAP) with mean percentages), pollen concentration (PC), and definition of lower boundaries (LB).

PAZ	Depth (m) & Age (ka BP)	Mean resolution	Pollen assemblage
II1	92.35–95.99 14.2–15.4	46 cm 177 years	AP: 16.8%; <i>Quercus ithaburensis</i> type (13.4%). NAP: 83.2%; Amaranthaceae (39.6%), Poaceae wild type (13.5%), Artemisia (9.6%), Tubuliflorae (4.8%), Rumex (2.4%), Apiaceae (2.4%), Liguliflorae (1.6%), Brassicaceae (1.6%), <i>Plantago</i> (1.5%), Cerealia type (1.4%). PC: Low (\circ 29,295 grains/cm 3); 3 gypsum samples. LB: Increase of Amaranthaceae, Tubuliflorae, Liguliflorae, Rumex; Decrease of Artemisia, <i>Quercus ithaburensis</i> type, <i>Juniperus</i> type.
II2a	95.99–114.56 15.4–30.6	47 cm 377 years	AP: 22.6%; <i>Quercus ithaburensis</i> type (15.2%), <i>Juniperus</i> type (4.7%), <i>Quercus calliprinos</i> type (1.1%). NAP: 77.4%; Artemisia (26.7%), Amaranthaceae (26.6%), Poaceae wild type (11.6%), Apiaceae (3.0%), Cerealia type (2.3%), Tubuliflorae (1.8%). PC: Low (\circ 33,382 grains/cm 3); 2 gypsum samples. LB: Increase of <i>Juniperus</i> type; Decrease of <i>Quercus ithaburensis</i> type, <i>Pistacia</i> .
II2b	114.56–130.99 30.6–34.7	131 cm 345 years	AP: 27.4%; <i>Quercus ithaburensis</i> type (21.3%), <i>Juniperus</i> type (3.3%), <i>Quercus calliprinos</i> type (1.0%). NAP: 72.6%; Artemisia (27.3%), Amaranthaceae (22.9%), Poaceae wild type (10.5%), Apiaceae (2.1%), Cerealia type (2.8%), Tubuliflorae (1.5%). PC: Low to moderate (\circ 49,362 grains/cm 3); no gypsum samples. LB: Increase of Artemisia; Decrease of <i>Plantago</i> .
II3	130.99–168.05 34.7–62.6	55 cm 404 years	AP: 29.9%; <i>Quercus ithaburensis</i> type (23.7%), <i>Juniperus</i> type (3.0%), <i>Quercus calliprinos</i> type (1.1%). NAP: 70.1%; Amaranthaceae (24.6%), Artemisia (22.9%), Poaceae wild type (10.5%), Cerealia type (2.0%), Tubuliflorae (1.7%), Apiaceae (1.6%), <i>Plantago</i> (1.0%). PC: Moderate (\circ 54,642 grains/cm 3); 4 gypsum samples. LB: Increase of <i>Quercus ithaburensis</i> type, Artemisia; Decrease of Amaranthaceae, <i>Plantago</i> , Liguliflorae.
II4	168.05–199.07 62.6–88.0	42 cm 345 years	AP: 23.6%; <i>Quercus ithaburensis</i> type (18.5%), <i>Juniperus</i> type (1.6%), <i>Pistacia</i> (1.5%). NAP: 76.4%; Amaranthaceae (31.2%), Artemisia (14.5%), Poaceae wild type (13.2%), Tubuliflorae (2.6%), <i>Plantago</i> (2.5%), Cerealia type (2.1%), Liguliflorae (1.9%), Brassicaceae (1.6%), Apiaceae (1.5%), Rumex (1.4%). PC: Moderate to high (\circ 62,087 grains/cm 3); 2 gypsum samples. LB: Not defined (end of record).

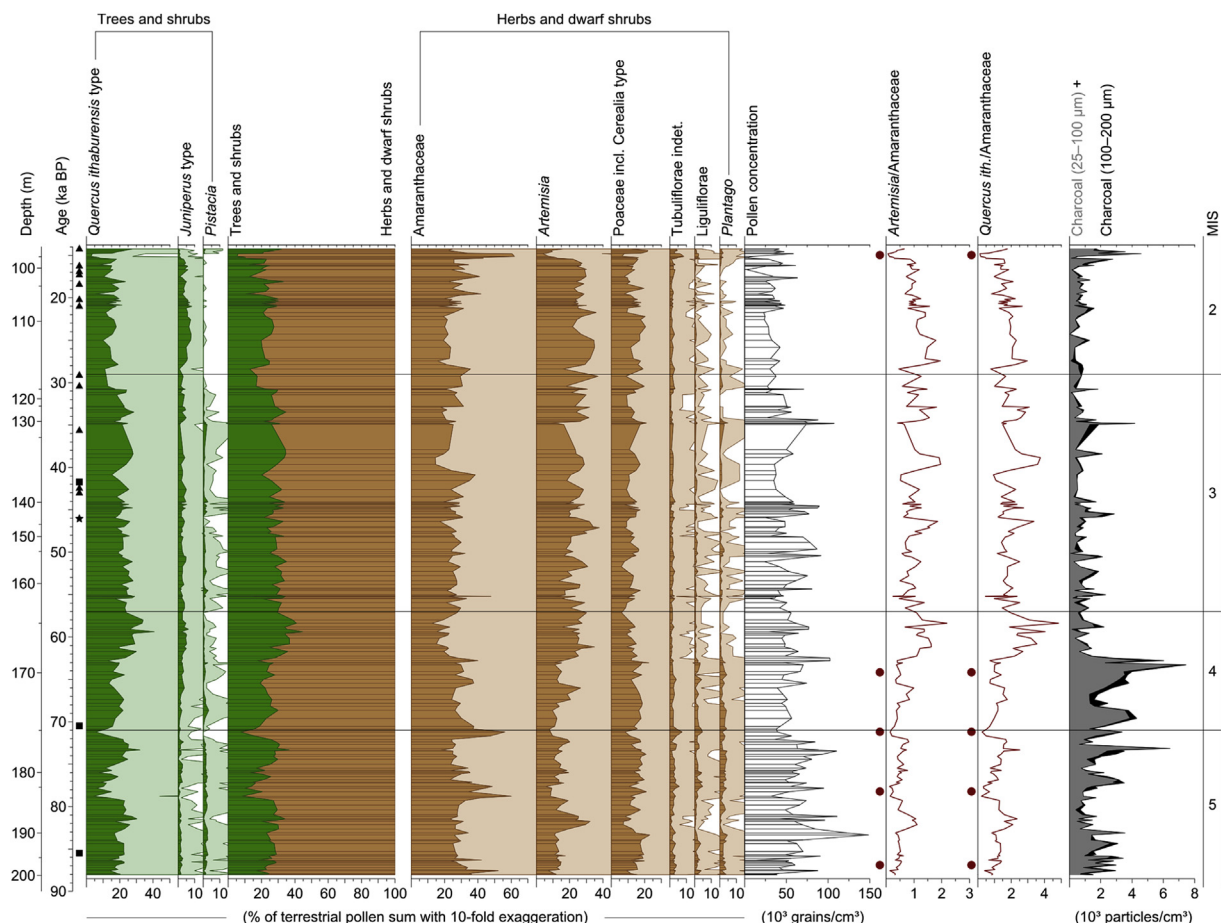


Fig. 6. Pollen diagram of Dead Sea core 5017-1-A plotted against age with selected taxa, pollen concentrations, ratios of *Artemisia* to Amaranthaceae and *Quercus ithaburensis* type to Amaranthaceae with dots marking dry events, charcoal concentrations, and marine isotope stages (MIS) after Lisicki and Raymo (2005). The chronology is based on a linear interpolation of calibrated radiocarbon dates (triangles), Uranium–Thorium dates (squares), and a correlated Uranium–Thorium date (star).

pollen type, which can morphologically be distinguished. While the wild type refer to the majority of wild grasses, the Cerealia type contain mainly domesticated cereals and their ancestors, which are native to this region (Beug, 2004).

Trees and shrubs never dominated the Dead Sea region during the investigated period. Nevertheless, they contributed substantially to the pollen composition (averagely 25.5%). *Quercus ithaburensis* type (deciduous oak) was the most abundant arboreal pollen type, followed by *Juniperus* type (juniper and/or Mediterranean cypress), *Quercus calliprinos* type (evergreen oak), and *Pistacia* (pistachio). While deciduous and evergreen oaks are usually well represented to overrepresented (van Zeist et al., 1975; Rossignol-Strick, 1995), *Pistacia* and *Juniperus* type are usually underrepresented in the pollen precipitation (Rossignol-Strick, 1995; van Zeist et al., 2009). All of these trees and shrubs represent the Mediterranean biome (Baruch, 1986; Litt et al., 2012), which occurs nowadays in the most humid areas of the southern Levant (Zohary, 1962). Modern Levantine vegetation studies indicated that a reduction of arboreal vegetation coincides with a decline in moisture (Zohary, 1962; Kadmon and Danin, 1999). Likewise, the Mediterranean biome retreats under reduced precipitation rates in the biome model (Figs. 3 and 4). This relation has also been described and discussed by Litt et al. (2012) based on botanical-climatological transfer functions by using a Holocene Dead Sea pollen record. Therefore, the amount of arboreal pollen is strongly related to changes in available moisture for plants in the past, i.e., effective moisture, which depends mainly on precipitation and evapotranspiration (the sum of evaporation and plant transpiration). The Q/A ratio – directly comparing the most abundant components of the Mediterranean and Saharo-Arabian biomes – also mainly reflects moisture changes. In addition, temperature reductions can limit the Mediterranean biome distribution, particularly at high altitudes (Figs. 3 and 4). Still, other factors such as seasonality, local habitats, and insolation must be considered for evaluating vegetation changes through time.

Pollen concentrations generally indicate vegetation density and pollen productivity in the lake catchment. However, Dead Sea samples that contain gypsum show low pollen concentrations, as indicated in Fig. 5, because gypsum laminae have higher sedimentation rates than alternating aragonite-detritus laminae (Stein, 2001; Torfstein et al., 2015). Still, the overall decreasing trend in pollen concentrations along the record suggests a stepwise vegetation density reduction, particularly at the MIS 5/4 transition and at ca. 35 ka BP.

The analysis of charred particles in sediments is one of the primary methods to reconstruct fire activity, i.e., fire frequency and/or fire intensity, in the past. The comparison with pollen assemblages allowed insights into the relationship between fire, vegetation, and climate (e.g., Swain, 1973; Daniau et al., 2010; Vannière et al., 2011). Charcoal particles above 100 µm in size are not transported far from fire sources. Thus, they indicate local fires. Smaller charcoal particles are able to travel longer distances and therefore reflect regional fires (Whitlock and Larsen, 2001). Charcoal concentrations in the investigated Dead Sea sediments vary from 0 to 7457 particles/cm³ (1476 particles/cm³ on average). Still, the highest charcoal concentrations are several times lower than during the last interglacial (Chen and Litt, 2018). Charcoal particles <100 µm constitute 84.6% of the charcoal sum and indicate the prevalence of regional fires.

Different fire regimes are generally generated by atmospheric conditions, ignition agents, and the availability of consumable resources, i.e., vegetation (Moritz et al., 2010). According to Whitlock et al. (2010), the highest fire activity is usually related to grassland and savanna biomes. Daniau et al. (2010) reviewed changes in fire regimes during the last glacial on a global scale and concluded that

they were primarily related to changes in plant productivity. Also previous studies from the Mediterranean and Near East that investigated the fire history during the last glacial connected enhanced fire activity to higher arboreal pollen percentages and an increased terrestrial biomass caused by higher temperatures and increased moisture (e.g., Daniau et al., 2007; Turner et al., 2010; Pickarski et al., 2015). In contrast, the results from the Dead Sea suggest that forest density, grassland occurrence, and thus availability of fuel was not the primary trigger for changes in fire activity because there is neither a significant linear correlation between charcoal concentrations and arboreal pollen percentages nor with Poaceae percentages. Hence, other climate variations are possible factors that primarily influenced the Dead Sea charcoal record. Such climate variations could be, for instance, longer/more intensive summer droughts (Vannière et al., 2008).

4.3.2. Rapid paleoenvironmental changes during late MIS 5 and early MIS 4

PAZ II4 (199.07–168.05 m; 88.0–62.6 ka BP) corresponds to MIS 5b/a and early MIS 4. An open vegetation with a variety of herbs and dwarf shrubs prevailed (Figs. 5 and 6). Amaranthaceae accompanied by *Artemisia* and Poaceae were important elements of the vegetation. Various herbaceous taxa further contributed to the composition of the vegetation, namely *Tubuliflorae*, *Liguliflorae* (both composites), *Plantago* (plantain), *Rumex* (dock), Brassicaceae (crucifers), and Apiaceae (umbellifers). Moderate pollen frequencies of *Quercus ithaburensis* type and small pollen amounts of *Pistacia*, *Juniperus* type, and *Quercus calliprinos* type indicate the occurrence of Mediterranean woodland elements. Trees and shrubs did probably not occur in a closed forest belt but were patchily distributed in habitats with locally more available moisture. They most likely formed a mosaic with Irano-Turanian steppe components.

The charcoal record indicates a rapidly fluctuating fire frequency with an increasing trend (Figs. 6 and 7). Highest charcoal concentrations of the investigated period appear in this PAZ. The charcoal record supports unstable environmental conditions with a high but fluctuating fire activity.

Fluctuations in the vegetation indicate millennial-scale climate oscillations with four phases of reduced available moisture expressed by low A/A and low Q/A ratios (Figs. 6 and 7). They strikingly coincide with the deposition of gypsum (Figs. 5 and 7; Neugebauer et al., 2014). Neugebauer et al. (2016) correlated dry phases during the early last glacial derived from micro-facies analyses from the Dead Sea core 5017-1-A to cold phases in the North Atlantic, coinciding with stadial conditions (mostly cold and dry) in other Mediterranean records. Following this interpretation, the detected dry phases might correlate to Greenland stadials (Fig. 7; Rasmussen et al., 2014), i.e., pollen would show a Dansgaard-Oeschger signature. However, the current chronology does not allow a convincing correlation to single climate events of other paleorecords. Thus, the connection between rapid vegetation changes in the Dead Sea region and high latitude climatic conditions during this phase remains speculative.

4.3.3. The environment during late MIS 4 to MIS 3 and implications for modern humans

PAZ II3 (168.05–130.99 m; 62.6–34.7 ka BP) corresponds to late MIS 4 and early/middle MIS 3. The onset of PAZ II3 marks the strongest shift in the vegetation during the investigated time, as indicated by the cluster analysis (Fig. 5). *Artemisia* pollen percentages increase while the pollen frequencies of a range of other herbs and dwarf shrubs, namely Amaranthaceae, Poaceae, *Tubuliflorae*, *Plantago*, *Liguliflorae*, Brassicaceae, and *Rumex*, decline. The change in non-arboreal pollen is also indicated by increased A/A values

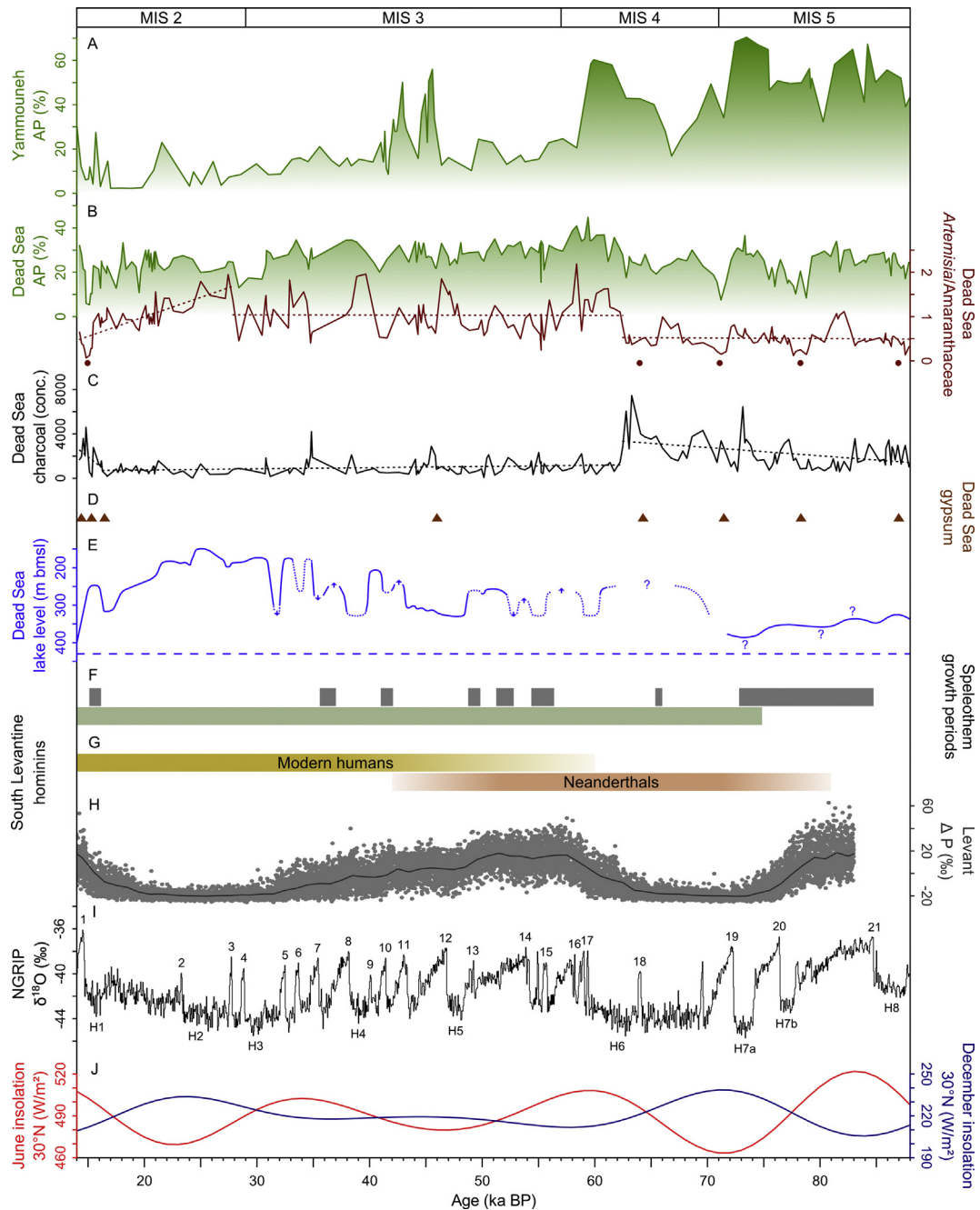


Fig. 7. Correlation of A) AP (arboreal pollen) from Yammounéh, Lebanon (Gasse et al., 2011, 2015), B) AP and *Artemisia/Amaranthaceae* ratios with dashed trend lines and dots marking dry events from Dead Sea (this study), C) charcoal concentrations in particles/cm³ with dashed trend lines from Dead Sea (this study), D) gypsum deposits in Dead Sea core 5017-1-A (Neugebauer et al., 2014), E) Dead Sea lake-level reconstructions (Waldmann et al., 2009; Torfstein et al., 2013b) with today's lake level (dashed line), F) speleothem growth periods from Mizpe Shelagim Cave, Mt. Hermon (above; Ayalon et al., 2013) and several caves west of the Dead Sea (below; Vaks et al., 2003; Lisker et al., 2010), G) south Levantine hominin record (Shea, 2008; Herskovitz et al., 2015), H) precipitation anomaly for the Levant expressed as percental deviation from total mean (today has a value of ca. 18%) with average in dark grey (Stockhecke et al., 2016), I) Greenland ice core isotope record with numbered Dansgaard-Oeschger events above (Rasmussen et al., 2014) and numbered Heinrich events below (Seierstad et al., 2014), and J) June and December insolation for the 30th parallel north (Berger and Loutre, 1991). Marine isotope stages (MIS) refer to Lisiecki and Raymo (2005).

(Fig. 6). Moreover, the onset of PAZ II3 displays an increase of arboreal pollen. Overall highest mean percentages of *Quercus ithaburensis* type occur in PAZ II3. The pollen composition mirrors a spread of *Artemisia* steppe and Mediterranean woodland components dominated by deciduous oak, implying an increase of available moisture for plants compared to earlier phases. **PAZ II2b (130.99–114.56 m; 34.7–30.6 ka BP)** corresponds to late MIS 3. Its vegetation composition and abundance of single taxa largely

resemble PAZ II3. However, *Artemisia* percentages further increase in PAZ II2b. The abundance of *Artemisia* is not only associated with an increase of effective moisture but can also be indicative for reduced temperatures. The complete absence of thermophilous *Olea europaea* (olive tree) in PAZ II2b – although never represented by high numbers in the pollen record – supports the latter explanation. A reduction of temperatures since ca. 35 ka BP coincides with the study by Ayalon et al. (2013) suggesting conditions too

cold for speleothem growth at Mt. Hermon, northern Israel, between ca. 35 and 16 ka BP (Fig. 7). During late MIS 4 and MIS 3, both factors – relatively high moisture availability and cool conditions – probably played an important role for the environment.

The charcoal record supports an environmental shift around 63–62 ka BP. The fire activity became low and stayed low until the late glacial. A possible trigger could be weaker/shorter summer droughts due to cooler and/or moister summer conditions.

Our observation of high effective moisture during late MIS 4 and MIS 3 is supported by the deposition of speleothems in areas that were too dry for speleothem growth during the Holocene, namely the rain shadow semi-desert and the northern Negev (Fig. 7; Vaks et al., 2003, 2006; Lisker et al., 2010; Bar-Matthews et al., 2017), and the continuous deposition of aad laminae in the Dead Sea core 5017-1-A (lithology in Fig. 5; Kagan et al., 2018) indicating a positive freshwater balance (e.g., Stein et al., 1997). Therefore, we cannot support the hypothesis that MIS 3 was a dry phase, as suggested by several authors who correlated warmer phases (e.g., Holocene, MIS 3) at the North Atlantic with drier phases in the southern Levant (e.g., Bartov et al., 2003; Haase-Schramm et al., 2004; Stein et al., 2010). Likewise, our palynological results contradict a previous vegetation model (Horowitz, 1992) that suggested the reduction of woodland components in the Dead Sea region during MIS 3. This discrepancy might be ascribed to the nature of MIS 3. Although defined as a separate isotope stage in the marine realm, the benthic $\delta^{18}\text{O}$ values defining MIS 3 are much higher than during full interglacial stages such as MIS 5e and 1, and therefore they are rather similar to the full glacial MIS 4 and 2 (Lisicki and Raymo, 2005). In addition, MIS 3 is not expressed as an interglacial as defined by Jessen and Milthers (1928) for terrestrial records.

To test which climate might have caused the described vegetation pattern with large proportions of steppe though still allowing enough moisture for Mediterranean woodland, we modeled the biome distribution in the Levant for MIS 3 given two different climate scenarios in the literature: a temperature reduction of 3 °C (see section 4.1) with I) a precipitation decrease of 15% following Stockhecke et al. (2016) (Fig. 4b) and II) a precipitation increase of 100% following Enzel et al. (2008) and Vaks et al. (2006) (Fig. 4c). Both model outputs fit very well with vegetation reconstructions for the Yammouneh Basin (Fig. 7; Gasse et al., 2011, 2015), indicating a sparse herbaceous flora in nowadays forested areas of Lebanon. However, the biome model reveals much different vegetation patterns for the Dead Sea region. Scenario I suggests a well-mixed balance of the three biome types with an increased probability for the Irano-Turanian biome compared to today. In contrast, scenario II suggests a strong expansion of the Mediterranean biome, causing lower probabilities of the other two biomes. The pollen signal from the Dead Sea (Fig. 6) supports the first scenario due to high proportions of Irano-Turanian taxa and moderate amounts of Mediterranean taxa. The model indicates that a small reduction in precipitation together with reduced temperatures does still allow sufficient moisture availability for the growth of Mediterranean taxa in the Dead Sea region.

The comparison of the Dead Sea region to northern latitudes reveals a contrasting pattern during late MIS 4 and MIS 3. Greenland and Europe were influenced by frequent and rapid climate fluctuations (Fig. 7; Rasmussen et al., 2014), causing rapid expansion and contraction of arboreal vegetation over southern Europe (e.g., Fletcher et al., 2010). In comparison to that, the Dead Sea region saw more stable environmental conditions with very low fire activity, with steady woodland occurrence (lowest AP standard deviation of the record), and without pronounced dry phases resulting in constant moisture availability. Still, climate tracers such as the pollen ratios A/A and Q/A indicate some

variations in the pollen assemblage that might refer to Dansgaard-Oeschger oscillations, as discussed above.

AMH occupied the southern Levant during this stable climate phase after an absence of several thousand years. Earlier dispersals from Africa into the southern Levant were dated to 194–177 ka BP based on fossils from the Misliya Cave, northern Israel (Hershkovitz et al., 2018), and to ca. 130–90 ka BP based on human remains from the Skhul Cave and the Qafzeh Cave, northern Israel (e.g., Valladas et al., 1988; Mercier et al., 1993; Grün et al., 2005). The fossils from the Misliya Cave provide the earliest evidence for AMH outside Africa (Hershkovitz et al., 2018). The oldest fossils from the investigated last glacial period date to 54.7 ± 5.5 ka BP and were excavated in the Manot Cave in northern Israel (Hershkovitz et al., 2015). Hershkovitz et al. (2015) suggested that those people could be closely related to the first AMH who eventually dispersed into Europe. Earliest evidence for the colonization of Europe by AMH dates to 45–43 ka BP (Benazzi et al., 2011).

AMH might have benefited from a humid phase between ca. 56 and 44 ka BP when crossing the nowadays arid regions between northeastern Africa and the southern Levant (Langgut et al., 2018). After entering the southern Levant, however, AMH lived in a refugial area with favorable environmental conditions on longer time scales according to our study. The vegetation formed a mosaic of Irano-Turanian steppe with herbs and dwarf shrubs, open Saharo-Arabian desert vegetation, and Mediterranean woodland elements. This diverse landscape offered a large variety of habitats for animals and humans. No pronounced dry phases occurred, and water was constantly available in the ecosystem. Temperatures were certainly lower than today, but the continuous occurrence of frost-sensitive *Pistacia* indicates mild winters, at least at lower altitudes (Rossignol-Strick, 1995). The fire activity was constantly very low, suggesting weak/short summer droughts.

In contrast, Neanderthals had already occupied the southern Levant since the late MIS 5. Neanderthal remains from the Amud, Kebara, and Geula Caves were dated to ca. 81–42 ka BP (Shea, 2008 and references therein). Thus, they already lived in the southern Levant during a climatically dynamic phase with pronounced dry phases, higher fire activity, and intensified resource uncertainty.

To conclude, Neanderthals tolerated a wide spectrum of environmental conditions in the glacial Dead Sea region, and diverse and rather stable environmental conditions since ca. 63 ka BP provided great potential for the residence of AMH.

4.3.4. Levantine vegetation pattern during MIS 2

PAZ II2a (114.56–95.99 m; 30.6–15.4 ka BP) corresponds to MIS 2. An important ecological change occurred within arboreal components at the MIS 3/2 transition. While thermophilous deciduous oaks became less abundant, *Juniperus* and/or *Cupressus sempervirens* (*Juniperus* type) spread (Figs. 5 and 6). A virtual absence of frost-sensitive *Pistacia* pollen point to reduced winter temperatures in areas where *Pistacia* had previously grown (Rossignol-Strick, 1995). Together with the high abundance of *Artemisia* and the complete absence of *Olea europaea*, these changes in the pollen assemblage indicate the coolest phase of the investigated timeframe. This conclusion fits well with temperature calculations inferred from the Soreq Cave speleothems, central Israel (McGarry et al., 2004; Affek et al., 2008) and alkenone-based sea surface temperatures for the southeastern Levantine Basin (Almogi-Labin et al., 2009). Low pollen concentrations suggest a sparser vegetation compared to previous phases.

The constantly low fire frequency, as indicated by low charcoal concentrations, coincides with observations by Orland et al. (2012). They suggested a decreased seasonal rainfall gradient prior to 15 ka BP inferred from the Soreq Cave speleothems. After 15 ka BP and particularly during the Holocene, the climatic conditions were

characterized by higher seasonality with distinct wet and dry seasons.

The comparison of pollen records from the Yammouneh Basin in Lebanon (Gasse et al., 2011, 2015), the Birkat Ram maar lake on the Golan Heights (Schiebel, 2013), the Sea of Galilee in northern Israel (Miebach et al., 2017; Schiebel and Litt, 2018), and the Dead Sea (Litt et al., 2012; this study) allows an assessment on vegetation and climate pattern in the Levant during MIS 2. The Yammouneh Basin and the Birkat Ram are located in regions that are nowadays characterized by Mediterranean climate with a climax of dense Mediterranean woodland. The Sea of Galilee lies at the southern edge of the Mediterranean biome bordering the Irano-Turanian steppe. The Dead Sea is located in a hyperarid area, where Saharo-Arabian desert vegetation prevails. The surrounding mountains are covered by Irano-Turanian steppe vegetation and Mediterranean woodland. Strong gradients in precipitation, temperature, and the vegetation distribution between these localities occur nowadays (Fig. 2; Zohary, 1962) and occurred during the Holocene (Fig. 8).

In contrast, Mediterranean forests were considerably reduced in the vicinity of the Yammouneh Basin, the Birkat Ram, and the Sea of Galilee during MIS 2. Arboreal components were more abundant in the Dead Sea region compared to the Holocene. However, a continuous and strong human impact, reducing the amount of trees and shrubs, has to be considered for the Holocene (Miller, 1991; Rollefson and Köhler-Rollefson, 1992), also given that mean arboreal percentages for the last interglacial optimum were more than twice as high as for the Holocene (Litt et al., 2012; Chen and Litt, 2018). Dwarf shrubs, grasses, and other herbs dominated the glacial vegetation in the whole study area, and there was no continuous and dense vegetation belt of the Mediterranean biome in the northern parts. Thermophilous trees were probably patchily distributed at moister habitats, particularly in the Jordan Rift Valley, where arboreal pollen percentages are somewhat higher than in the mountainous areas of the north.

The comparison of the described vegetation pattern with modeled biome distributions (Fig. 4) enables us to evaluate two different climate scenarios: a temperature reduction of 6 °C (see section 4.1) with I) a precipitation decrease of 30% following Stockhecke et al. (2016) (Fig. 4d) and II) a precipitation increase of 100% following Enzel et al. (2008) and Vaks et al. (2006) (Fig. 4e). Both model outputs fit well with the pollen data from Yammouneh and Birkat Ram, suggesting the dominance of steppe and reduction of forest during MIS 2. However, the vegetation patterns differ greatly in the Dead Sea region: While scenario I triggers a similar distribution of the Mediterranean biome with lower probabilities of occurrence, scenario II suggests a spread of Mediterranean woodland into regions close to the Dead Sea that are nowadays arid. While scenario I slightly underestimates the proportion of Mediterranean woodland compared to the Dead Sea pollen data, scenario II clearly overestimates the distribution of the Mediterranean biome. Further studies are needed to estimate precipitation rates for MIS 2, which were probably slightly reduced but by not as much as 30%. In addition, precise temperature estimations, particularly for interior regions such as the Jordan Rift Valley, are needed because temperature also modifies the biome distribution.

Slightly lowered precipitation rates during MIS 2 could have still allowed relatively high available moisture for plants and a positive freshwater balance in the Dead Sea region. Reduced temperatures (Fig. 7; Rasmussen et al., 2014), low summer insolation (Figs. 7 and 8; Berger and Loutre, 1991), and reduced catchment wide evaporation (due to lower temperatures and higher relative humidity; Bar-Matthews et al., 2017) would cause higher effective moisture compared to recent conditions. The total evapotranspiration would have been additionally lowered because of the low woodland cover

in the northern mountain range, leading to reduced plant transpiration. This can have a significant impact on the water budget (Schiller et al., 2002, 2010; Ungar et al., 2013). A lower basin wide evaporation and lower plant transpiration would have still allowed a positive freshwater balance in the lakes, leading to the increased lake levels even under reduced precipitation rates (Stockhecke et al., 2016). In addition, plant cover could have been shaped by available water in their habitats, while additional precipitation was stored as snow on high mountains (Robinson et al., 2006) and released as flash floods. The frequency of flash floods was considerably increased during rising Lake Lisan levels (Ben Dor et al., 2018). Plants could probably not sufficiently use the water brought by rapid snowmelts in springs and rapid drains during flash floods. Moreover, plant growth could have been limited by reduced atmospheric CO₂ levels during the last glacial, as previous studies suggested (e.g., Cowling and Sykes, 1999; Prentice et al., 2017). According to experimental studies, low CO₂ can result in decreased plant fitness and increased water use, especially of C3 plants (Gerhart and Ward, 2010 and references therein). Therefore, a reduction of forests and a shift from C3 plant to C4 plant dominance were ascribed to low CO₂ levels in other regions (e.g., Levis et al., 1999; Harrison and Prentice, 2003). However, a correlation of woodland retreat and a spread of C4 plants (e.g., many Amaranthaceae species) with gradually decreasing atmospheric CO₂ levels during the last glacial (Petit et al., 1999) cannot be detected in the Dead Sea pollen record. Therefore, the impact of CO₂ on the Levantine vegetation composition seems to be limited. Still, decreasing CO₂ levels could explain the gradually shrinking pollen concentration that indicates a declining vegetation density.

4.3.5. Preliminary insights into the late glacial environment

PAZ III (95.99–92.35 m; 15.4–14.2 ka BP) corresponds to part of the late glacial. The phase begins with a pronounced peak of Amaranthaceae and a small peak of Asteraceae (Tubuliflorae and Liguliflorae). Simultaneously, most other taxa drop. Thereafter, the composition and abundance of taxa resembles PAZ II4 with a diverse herbaceous flora and low amounts of *Artemisia*. It is probable that the initial peaks of Amaranthaceae and Asteraceae reflect a local spread of pioneer plants, engendering a temporal overrepresentation in the pollen assemblage and a statistical suppression of other taxa. A spread of local plants is supported by a simultaneous major lake-level drop of Lake Lisan from ca. 260–465 m bmsl, one of the lowest stands during the Late Quaternary (Fig. 7; Stein et al., 2010; Torfstein et al., 2013b). The exposed shores could have been vegetated by saline-tolerant pioneer communities including species of Amaranthaceae and Asteraceae, as modern observations suggest (Aloni et al., 1997). Due to the wind-pollination of Amaranthaceae, local stands of this family are particularly overrepresented in the pollen diagram. A similar peak was observed after a strong lake-level decline at the Sea of Galilee at ca. 24–23 ka BP (Miebach et al., 2017), and the same phenomenon probably played a role at the Dead Sea during the transition to the last interglacial period (Chen and Litt, 2018). Still, a short dry period, as suggested by the deposition of gypsum in the Dead Sea core 5017-1-A (Figs. 5 and 7; Torfstein et al., 2013b; Neugebauer et al., 2014), and the strong lake-level reduction of Lake Lisan (Fig. 7; Torfstein et al., 2013b) most likely additionally triggered the spread of herbs and dwarf shrubs.

Frost-sensitive *Pistacia* and *Olea europaea* occur consistently again after a virtual absence of many millennia. This indicates a return to higher temperatures at least during winters (van Zeist et al., 1975; Rossignol-Strick, 1995). The reduction of *Artemisia* and *Juniperus* type, which were common during the cold MIS 2 including the Last Glacial Maximum, also imply higher temperatures compared to MIS 2.

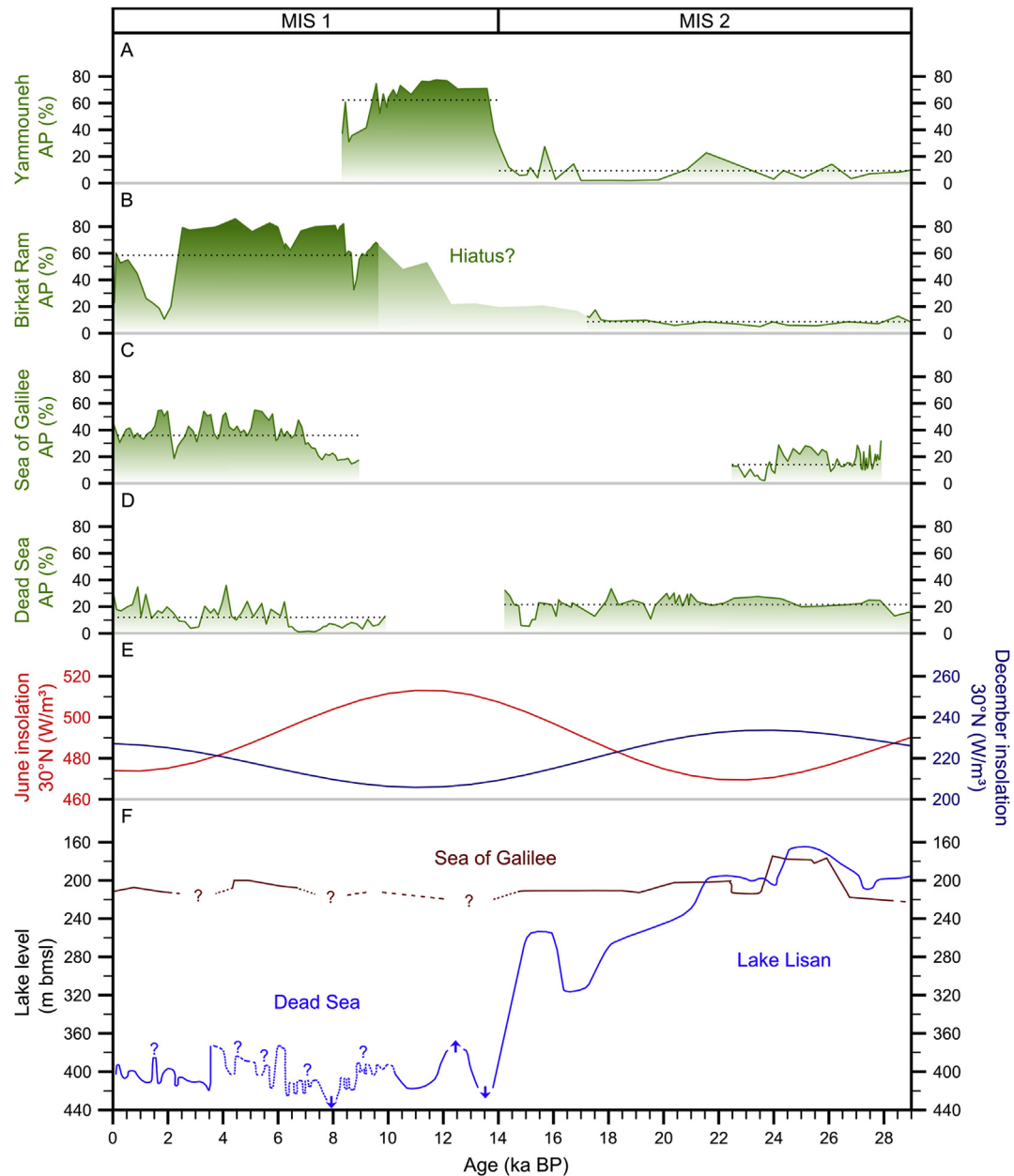


Fig. 8. Comparison of a north-to-south gradient in the Levant. Arboreal pollen (AP) with mean percentages shown as dashed lines from A) Yammouneh, Lebanon (Gasse et al., 2011, 2015), B) Birkat Ram, Golan Heights (Schiebel, 2013; discontinuous sedimentation might occur between ca. 10 and 17 ka BP), C) Sea of Galilee, northern Israel (MIS 1: Schiebel and Litt, 2018; MIS 2: Miebach et al., 2017), and D) Dead Sea, Israel/Palestine/Jordan (MIS 1: Litt et al., 2012; MIS 2: this study). E) June and December insolation for the 30th parallel north (Berger and Loutre, 1991). F) Lake-level reconstructions of the Sea of Galilee (Hazan et al., 2005), the Dead Sea, and its precursor Lake Lisan (Torfstein et al., 2013b). Marine isotope stages (MIS) refer to Lisiecki and Raymo (2005).

Since ca. 16.2 ka, the fire activity increased again. A probable cause could be a higher seasonality with distinct wet and dry seasons. This explanation is in line with the study by Orland et al. (2012), suggesting an increased seasonality since the late glacial inferred from the Soreq Cave speleothems.

5. Summary and conclusions

The 5017-1 profile obtained by the DSDDP is the longest continuous sediment record from the Dead Sea Basin, enabling the detailed reconstruction of the southern Levantine environmental history (Neugebauer et al., 2014). The detailed vegetation history of the southern Levant in particular was still insufficient understood

given the scarceness of long continuous lacustrine sediment sequences and major chronological uncertainties in many pollen records (e.g., Rossignol-Strick, 1995; Weinstein-Evron et al., 2001; Meadows, 2005). Here, we analyzed the pollen and microscopic charcoal assemblage of the Lisan Formation of the Dead Sea core 5017-1-A, spanning ca. 88–14 ka BP. Moreover, we performed biome modeling to assess shifts in biome distribution in response to climate variations. The biome modeling results illustrate the climate sensitivity of the regional vegetation and help to evaluate climate scenarios for the last glacial Levant.

The pollen record indicates a mixture of Irano-Turanian steppe, Saharo-Arabian desert vegetation, and Mediterranean woodland elements. Although changes in the pollen composition might not

provide clear evidence for variations in the precipitation amount, it indicates the availability of water for plants, i.e., the effective moisture. Decreased pollen ratios of AP/NAP, A/A, and Q/A indicate low effective moisture probably pointing to a Dansgaard-Oeschger signature. Hence, four dry phases occurred during the early last glacial (MIS 5b/a and early MIS 4), which coincide with the deposition of gypsum in Lake Lisan. A high and dynamic fire activity took place.

An increased proportion of Irano-Turanian steppe vegetation and Mediterranean woodland elements suggests consistently high effective moisture during late MIS 4, MIS 3, and MIS 2, when fire activity was continuously low. Biome modeling suggests that no precipitation increase is needed for such amounts of effective moisture. Lower insolation, reduced catchment wide evapotranspiration, and low temperatures were probably sufficient for a positive water balance. MIS 2 was the coolest period of the investigated timeframe, as indicated by a change in arboreal taxa.

The residence of anatomically modern humans in the southern Levant during the last glacial was supported by stable environmental conditions with relatively high effective moisture and low fire activity. In contrast, Neanderthals had already lived in a dynamic ecosystem with changing water availability and higher fire activity, thus tolerating a wide spectrum of environmental conditions.

The comparison of Levantine pollen records along a north-to-south gradient indicates that, at least during MIS 2, there was no gradient of available water for plants comparable to the Holocene and today. An overall more similar, open vegetation occurred, and there was no dense Mediterranean woodland belt in the north. Scattered stands of thermophilous woodland components – particularly found at lower altitudes such as the Jordan Rift Valley – formed a heterogeneous landscape.

Major environmental changes occurred during the late glacial. However, further high-resolution analyses based on a robust chronology are needed to reveal the detailed vegetation and fire history.

The new palynological record contributes towards our understanding of the influence of long-term and short-term climate oscillations on the environment. New insights into the Levantine vegetation history help to reconstruct and evaluate the regional paleoclimate, which also carries implications for recent and future climate changes. Furthermore, the detailed knowledge of the environmental setting is essential to reveal the relationship between environmental developments and anthropogenic processes in the past.

Data availability

The palynological dataset related to this article is available on the PANGAEA database (<https://doi.pangaea.de/10.1594/PANGAEA.900564>).

Acknowledgements

We thank the DSDDP participants for drilling, opening, and describing the Dead Sea cores. We acknowledge Nadine Pickarski, Chunzhu Chen, and Vera Schiebel for supporting the sampling and Karen Schmeling for supporting the pollen preparation. We thank Chunzhu Chen, Ina Neugebauer, Vera Schiebel, Laurence Vidal, Benno Thoma, Mona Stockhecke, and colleagues from DSDDP and CRC 806 for sharing their data and their expertise. This project is affiliated to the CRC 806 “Our way to Europe” (Project Number 57444011). We thank the German Research Foundation for funding this project. We also acknowledge two anonymous reviewers for the positive feedback and valuable suggestions to improve the

manuscript.

References

- Affek, H.P., Bar-Matthews, M., Ayalon, A., Matthews, A., Eiler, J.M., 2008. Glacial/interglacial temperature variations in Soreq cave speleothems as recorded by ‘clumped isotope’ thermometry. *Geochim. Cosmochim. Acta* 72, 5351–5360.
- Almogi-Labin, A., Bar-Matthews, M., Shriki, D., Kolosovsky, E., Paterne, M., Schilman, B., Ayalon, A., Aizenshtat, Z., Matthews, A., 2009. Climatic variability during the last ~90 ka of the southern and northern Levantine Basin as evident from marine records and speleothems. *Quat. Sci. Rev.* 28, 2882–2896.
- Aloni, E., Eshel, A., Waisel, Y., 1997. The botanical conquest of the newly exposed shores of the Dead Sea. In: Niemi, T.M., Ben-Avraham, Z., Gat, J.R. (Eds.), *The Dead Sea: the Lake and its Setting*. Oxford University Press, New York, Oxford, pp. 277–281.
- Ayalon, A., Bar-Matthews, M., Frumkin, A., Matthews, A., 2013. Last Glacial warm events on Mount Hermon: the southern extension of the Alpine karst range of the east Mediterranean. *Quat. Sci. Rev.* 59, 43–56.
- Bar-Matthews, M., Ayalon, A., Vaks, A., Frumkin, A., 2017. Climate and environment reconstructions based on speleothems from the levant. In: Enzel, Y., Bar-Yosef, O. (Eds.), *Quaternary of the Levant: Environments, Climate Change, and Humans*, Cambridge, pp. 151–164.
- Barkan, E., Luz, B., Lazar, B., 2001. Dynamics of the carbon dioxide system in the Dead Sea. *Geochim. Cosmochim. Acta* 65, 355–368.
- Bartov, Y., Goldstein, S.L., Stein, M., Enzel, Y., 2003. Catastrophic arid episodes in the eastern Mediterranean linked with the north Atlantic Heinrich events. *Geology* 31, 439–442.
- Bartov, Y., Stein, M., Enzel, Y., Agnon, A., Reches, Z., 2002. Lake levels and sequence stratigraphy of Lake Lisan, the late Pleistocene precursor of the Dead Sea. *Quat. Res.* 57, 9–21.
- Baruch, U., 1986. The late Holocene vegetational history of Lake Kinneret (Sea of Galilee). *Israel. Paléorient* 12, 37–48.
- Begin, Z.B., Ehrlich, A., Nathan, Y., 1974. Lake Lisan: the Pleistocene precursor of the Dead Sea. *Geol. Surv. Isr. Bull.* 1–30.
- Ben Dor, Y., Armon, M., Ahlborn, M., Morin, E., Erel, Y., Brauer, A., Schwab, M.J., Tjallingii, R., Enzel, Y., 2018. Changing flood frequencies under opposing late Pleistocene eastern Mediterranean climates. *Sci. Rep.* 8, 8445.
- Benazzi, S., Douka, K., Fornai, C., Bauer, C.C., Kullmer, O., Svoboda, J., Pap, I., Mallegni, F., Bayle, P., Coquerelle, M., Condemi, S., Ronchitelli, A., Harvati, K., Weber, G.W., 2011. Early dispersal of modern humans in Europe and implications for Neanderthal behaviour. *Nature* 479, 525–528.
- Berger, A., Loutre, M.F., 1991. Insolation values for the climate of the last 10 million years. *Quat. Sci. Rev.* 10, 297–317.
- Beug, H.-J., 2004. Leitfaden der Pollenbestimmung für Mitteleuropa und angrenzende Gebiete. Verlag Dr. Friedrich Pfeil, München.
- Birks, H.J.B., 1973. Past and Present Vegetation of the Isle of Skye. Cambridge University Press, Cambridge.
- Cheddadi, R., Rossignol-Strick, M., 1995. Eastern Mediterranean Quaternary paleoclimates from pollen and isotope records of marine cores in the Nile Cone Area. *Paleoceanography* 10, 291–300.
- Chen, C., Litt, T., 2018. Dead Sea pollen provides new insights into the paleoenvironment of the southern Levant during MIS 6–5. *Quat. Sci. Rev.* 188, 15–27.
- Cowling, S.A., Sykes, M.T., 1999. Physiological significance of low atmospheric CO₂ for plant–climate interactions. *Quat. Res.* 52, 237–242.
- Danius, A.L., Harrison, S.P., Bartlein, P.J., 2010. Fire regimes during the last glacial. *Quat. Sci. Rev.* 29, 2918–2930.
- Danius, A.L., Sánchez-Goni, M.F., Beaufort, L., Laggoun-Défarge, F., Loutre, M.F., Duprat, J., 2007. Dansgaard–Oeschger climatic variability revealed by fire emissions in southwestern Iberia. *Quat. Sci. Rev.* 26, 1369–1383.
- Danin, A., 1992. Flora and vegetation of Israel and adjacent areas. *Boccone* 3, 18–42.
- Danin, A., 1999. Desert rocks as plant refugia in the Near East. *Bot. Rev.* 65, 93–170.
- Danin, A., Plitmann, U., 1987. Revision of the plant geographical territories of Israel and Sinai. *Plant Systemat. Evol.* 156, 43–53.
- Dayan, U., Morin, E., 2006. Flash flood-producing rainstorms over the Dead Sea: a review. In: Enzel, Y., Agnon, A., Stein, M. (Eds.), *New Frontiers in Dead Sea Paleoenvironmental Research*. Geological Society of America, Boulder, pp. 53–62.
- Deville, A.L., Gasse, F., Vidal, L., Williamson, D., Demory, F., Van Campo, E., Ghaleb, B., Thouveny, N., 2011. A 250 ka sedimentary record from a small karstic lake in the Northern Levant (Yammoūneh, Lebanon): paleoclimatic implications. *Palaeogeogr. Palaeoclimatol. Palaeoecol.* 305, 10–27.
- El-Moslimany, A.P., 1990. Ecological significance of common nonarboreal pollen: examples from drylands of the Middle East. *Rev. Palaeobot. Palynol.* 64, 343–350.
- Enzel, Y., Amit, R., Dayan, U., Crouvi, O., Kahana, R., Ziv, B., Sharon, D., 2008. The climatic and physiographic controls of the eastern Mediterranean over the late Pleistocene climates in the southern Levant and its neighboring deserts. *Glob. Planet. Chang.* 60, 165–192.
- Enzel, Y., Bookman, R., Sharon, D., Gvirtzman, H., Dayan, U., Ziv, B., Stein, M., 2003. Late Holocene climates of the Near East deduced from Dead Sea level variations and modern regional winter rainfall. *Quat. Res.* 60, 263–273.
- Faegri, K., Iversen, J., 1989. *Textbook of Pollen Analysis*, 4 ed. John Wiley & Sons, Chichester, New York; Brisbane; Toronto; Singapore.

- Fleitmann, D., Cheng, H., Badertscher, S., Edwards, R.L., Mudelsee, M., Göktürk, O.M., Fankhauser, A., Pickering, R., Raible, C.C., Matter, A., Kramers, J., Tüysüz, O., 2009. Timing and climatic impact of Greenland interstadials recorded in stalagmites from northern Turkey. *Geophys. Res. Lett.* 36, L19707.
- Fletcher, W.J., Sánchez-Góñi, M.F., Allen, J.R.M., Cheddadi, R., Combourieu-Nebout, N., Huntley, B., Lawson, I., Londeix, L., Magri, D., Margari, V., Müller, U.C., Naughton, F., Novenko, E., Roucoux, K., Tzedakis, P.C., 2010. Millennial-scale variability during the last glacial in vegetation records from Europe. *Quat. Sci. Rev.* 29, 2839–2864.
- Garfunkel, Z., 1997. The history and Formation of the Dead Sea basin. In: Niemi, T.M., Ben-Avraham, Z., Gat, J.R. (Eds.), *The Dead Sea: the Lake and its Setting*. Oxford University Press, New York, Oxford, pp. 36–56.
- Garfunkel, Z., 2014. Lateral motion and deformation along the Dead Sea transform. In: Garfunkel, Z., Ben-Avraham, Z., Kagan, E. (Eds.), *Dead Sea Transform Fault System: Reviews*. Springer, Dordrecht, pp. 109–150.
- Gasse, F., Vidal, L., Develle, A.L., Van Campo, E., 2011. Hydrological variability in the Northern Levant: a 250 ka multiproxy record from the Yammouné (Lebanon) sedimentary sequence. *Clim. Past* 7, 1261–1284.
- Gasse, F., Vidal, L., Van Campo, E., Demory, F., Develle, A.-L., Tachikawa, K., Elias, A., Bard, E., García, M., Sonzogni, C., Thouveny, N., 2015. Hydroclimatic changes in northern Levant over the past 400,000 years. *Quat. Sci. Rev.* 111, 1–8.
- Gavrieli, I., Stein, M., 2006. On the origin and fate of the brines in the Dead Sea basin. In: Enzel, Y., Agnon, A., Stein, M. (Eds.), *New Frontiers in Dead Sea Paleoenvironmental Research*. Geological Society of America, Boulder, pp. 183–194.
- Gerhart, L.M., Ward, J.K., 2010. Plant responses to low [CO₂] of the past. *New Phytol.* 188, 674–695.
- Goldreich, Y., 2003. *The Climate of Israel: Observation, Research and Application*. Springer, New York.
- Greenbaum, N., Ben-Zvi, A., Haviv, I., Enzel, Y., 2006. The hydrology and paleohydrology of the Dead Sea tributaries. In: Enzel, Y., Agnon, A., Stein, M. (Eds.), *New Frontiers in Dead Sea Paleoenvironmental Research*. Geological Society of America, Boulder, pp. 63–93.
- Grimm, E.C., 1987. CONISS: a FORTRAN 77 program for stratigraphically constrained cluster analysis by the method of incremental sum of squares. *Comput. Geosci.* 13, 13–35.
- Grün, R., Stringer, C., McDermott, F., Nathan, R., Porat, N., Robertson, S., Taylor, L., Mortimer, G., Eggins, S., McCulloch, M., 2005. U-series and ESR analyses of bones and teeth relating to the human burials from Skhul. *J. Hum. Evol.* 49, 316–334.
- Haase-Schramm, A., Goldstein, S.L., Stein, M., 2004. U-Th dating of Lake Lisan (late Pleistocene Dead Sea) aragonite and implications for glacial east Mediterranean climate change. *Geochim. Cosmochim. Acta* 68, 985–1005.
- Harris, I., Jones, P.D., Osborn, T.J., Lister, D.H., 2014. Updated high-resolution grids of monthly climatic observations – the CRU TS3.10 Dataset. *Int. J. Climatol.* 34, 623–642.
- Harrison, S.P., Prentice, A.I., 2003. Climate and CO₂ controls on global vegetation distribution at the last glacial maximum: analysis based on palaeovegetation data, biome modelling and palaeoclimate simulations. *Glob. Chang. Biol.* 9, 983–1004.
- Hazan, N., Stein, M., Agnon, A., Marco, S., Nadel, D., Negendank, J.F.W., Schwab, M.J., Neev, D., 2005. The late quaternary limnological history of Lake Kinneret (Sea of Galilee), Israel. *Quat. Res.* 63, 60–77.
- Hershkovitz, I., Marder, O., Ayalon, A., Bar-Matthews, M., Yasur, G., Boaretto, E., Caracuta, V., Alex, B., Frumkin, A., Goder-Goldberger, M., Gunz, P., Holloway, R.L., Latimer, B., Lavi, R., Matthews, A., Slon, V., Mayer, D.B.-Y., Berna, F., Bar-Oz, G., Yeshurun, R., May, H., Hans, M.G., Weber, G.W., Barzilai, O., 2015. Levantine cranium from Manot Cave (Israel) foreshadows the first European modern humans. *Nature* 520, 216–219.
- Hershkovitz, I., Weber, G.W., Quam, R., Duval, M., Grün, R., Kinsley, L., Ayalon, A., Bar-Matthews, M., Valladas, H., Mercier, N., Arsuaga, J.L., Martín-Torres, M., Bermúdez de Castro, J.M., Fornai, C., Martín-Francés, L., Sarig, R., May, H., Krenn, V.A., Slon, V., Rodríguez, L., García, R., Lorenzo, C., Carretero, J.M., Frumkin, A., Shahack-Gross, R., Bar-Yosef Mayer, D.E., Cui, Y., Wu, X., Peled, N., Groman-Yaroslavski, I., Weissbrod, L., Yeshurun, R., Tsatskin, A., Zaidner, Y., Weinstein-Evron, M., 2018. The earliest modern humans outside Africa. *Science* 359, 456–459.
- Horowitz, A., 1979. *The Quaternary of Israel*. Academic Press, New York, London.
- Horowitz, A., 1992. *Palynology of Arid Lands*. Elsevier, Amsterdam.
- Jessen, K., Milthers, V., 1928. Stratigraphical and paleontological studies of interglacial fresh-water deposits in Jutland and northwest Germany. *Danmarks Geologiske Undersøgelse* 2, 1–379.
- Kadmon, R., Danin, A., 1999. Distribution of plant species in Israel in relation to spatial variation in rainfall. *J. Veg. Sci.* 10, 421–432.
- Kagan, E., Stein, M., Marco, S., 2018. Integrated paleoseismic chronology of the last glacial Lake Lisan: from Lake margin seismites to deep-lake mass transport deposits. *J. Geophys. Res.: Solid Earth* 123.
- Katz, A., Kolodny, Y., Nissenbaum, A., 1977. The geochemical evolution of the Pleistocene Lake Lisan-Dead Sea system. *Geochim. Cosmochim. Acta* 41, 1609–1626.
- Kitagawa, H., Stein, M., Goldstein, S.L., Nakamura, T., Lazar, B., 2017. Radiocarbon chronology of the DSDDP core at the deepest floor of the Dead Sea. *Radiocarbon* 59, 383–394.
- Kuhlwilm, M., Gronau, I., Hubisz, M.J., de Filippo, C., Prado-Martinez, J., Kircher, M., Fu, Q., Burbano, H.A., Lalueza-Fox, C., de la Rasilla, M., Rosas, A., Rudan, P., Brajkovic, D., Kucan, Ž., Gušić, I., Marques-Bonet, T., Andrés, A.M., Viola, B., Pääbo, S., Meyer, M., Siepel, A., Castellano, S., 2016. Ancient gene flow from early modern humans into Eastern Neanderthals. *Nature* 530, 429–433.
- Kushnir, Y., Dayan, U., Ziv, B., Morin, E., Enzel, Y., 2017. Climate of the levant: phenomena and mechanisms. In: Enzel, Y., Bar-Yosef, O. (Eds.), *Quaternary of the Levant: Environments, Climate Change, and Humans*. Cambridge University Press, Cambridge, pp. 31–44.
- Langgut, D., 2018. Late quaternary nile flows as recorded in the Levantine Basin: the palynological evidence. *Quat. Int.* 464, 273–284.
- Langgut, D., Almogi-Labin, A., Bar-Matthews, M., Pickarski, N., Weinstein-Evron, M., 2018. Evidence for a humid interval at ~56–44 ka in the Levant and its potential link to modern humans dispersal out of Africa. *J. Hum. Evol.* 124, 75–90.
- Langgut, D., Almogi-Labin, A., Bar-Matthews, M., Weinstein-Evron, M., 2011. Vegetation and climate changes in the South Eastern Mediterranean during the Last Glacial-Interglacial cycle (86 ka): new marine pollen record. *Quat. Sci. Rev.* 30, 3960–3972.
- Levis, S., Foley, J.A., Pollard, D., 1999. CO₂, climate, and vegetation feedbacks at the Last Glacial Maximum. *J. Geophys. Res.: Atmosphere* 104, 31191–31198.
- Lisiecki, L.E., Raymo, M.E., 2005. A Pliocene-Pleistocene stack of 57 globally distributed benthic $\delta^{18}\text{O}$ records. *Paleoceanography* 20, PA1003.
- Lisker, S., Vaks, A., Bar-Matthews, M., Porat, R., Frumkin, A., 2010. Late Pleistocene palaeoclimatic and palaeoenvironmental reconstruction of the Dead Sea area (Israel), based on speleothems and cave stromatolites. *Quat. Sci. Rev.* 29, 1201–1211.
- Litt, T., Ohlwein, C., Neumann, F.H., Hense, A., Stein, M., 2012. Holocene climate variability in the Levant from the Dead Sea pollen record. *Quat. Sci. Rev.* 49, 95–105.
- Machlus, M., Enzel, Y., Goldstein, S.L., Marco, S., Stein, M., 2000. Reconstructing low levels of Lake Lisan by correlating fan-delta and lacustrine deposits. *Quat. Int.* 73 (74), 137–144.
- Masson-Delmotte, V., Schulz, M., Abe-Ouchi, A., Beer, J., Ganopolski, A., González Rouco, J.F., Jansen, E., Lambeck, K., Luterbacher, J., Naish, T., Osborn, T., Otto-Bliesner, B., Quinn, T., Ramesh, R., Rojas, M., Shao, X., Timmermann, A., 2013. Information from paleoclimate archives. In: Stocker, T.F., Qin, D., Plattner, G.-K., Tignor, M., Allen, S.K., Boschung, J., Nauels, A., Xia, Y., Bex, V., Midgley, P.M. (Eds.), *Climate Change 2013: the Physical Science Basis. Contribution of Working Group I to the Fifth Assessment Report of the Intergovernmental Panel on Climate Change*. Cambridge University Press, Cambridge, New York, pp. 383–464.
- McGarry, S., Bar-Matthews, M., Matthews, A., Vaks, A., Schilman, B., Ayalon, A., 2004. Constraints on hydrological and paleotemperature variations in the Eastern Mediterranean region in the last 140ka given by the δD values of speleothem fluid inclusions. *Quat. Sci. Rev.* 23, 919–934.
- Meadows, J., 2005. The younger dryas episode and the radiocarbon chronologies of the lake Huleh and Ghab Valley pollen diagrams, Israel and Syria. *Holocene* 15, 631–636.
- Mellars, P., 2011. Palaeoanthropology: the earliest modern humans in Europe. *Nature* 479, 483–485.
- Mercier, N., Valladas, H., Bar-Yosef, O., Vandermeersch, B., Stringer, C., Joron, J.L., 1993. Thermoluminescence date for the Mousterian burial site of Es-Skhul, Mt. Carmel. *J. Archaeol. Sci.* 20, 169–174.
- Meusel, H., Jäger, E., Rauschert, S., Weinert, E., 1965. *Vergleichende Chorologie der zentraleuropäischen Flora*. Gustav Fischer-Verlag, Jena.
- Miebach, A., Chen, C., Schwab, M.J., Stein, M., Litt, T., 2017. Vegetation and climate during the Last Glacial high stand (ca. 28–22 ka BP) of the Sea of Galilee, northern Israel. *Quat. Sci. Rev.* 156, 47–56.
- Miller, N.F., 1991. The Near East. In: van Zeist, W., Wasylkowa, K., Behre, K.E. (Eds.), *Progress in Old World Palaeoethnobotany*. Balkema, Rotterdam, pp. 133–160.
- Moore, P.D., Webb, J.A., Collinson, M.E., 1991. *Pollen Analysis*, 2 ed. Blackwell Scientific Publications, Oxford.
- Moritz, M.A., Krawchuk, M.A., Parriesien, M.-A., 2010. Pyrogeography: understanding the ecological niche of fire. *PAGES News* 18, 83–85.
- Müller, U.C., Pross, J., Tzedakis, P.C., Gamble, C., Kotthoff, U., 2011. The role of climate in the spread of modern humans into Europe. *Quat. Sci. Rev.* 30, 273–279.
- Neugebauer, I., Brauer, A., Schwab, M.J., Waldmann, N.D., Enzel, Y., Kitagawa, H., Torfstein, A., Frank, U., Dulski, P., Agnon, A., Ariztegui, D., Ben-Avraham, Z., Goldstein, S.L., Stein, M., 2014. Lithology of the long sediment record recovered by the ICDP Dead Sea deep drilling project (DSDDP). *Quat. Sci. Rev.* 102, 149–165.
- Neugebauer, I., Schwab, M.J., Waldmann, N.D., Tjallingii, R., Frank, U., Hadzhilianova, E., Naumann, R., Taha, N., Agnon, A., Enzel, Y., Brauer, A., 2016. Hydroclimatic variability in the Levant during the early last glacial (~117–75 ka) derived from micro-facies analyses of deep Dead Sea sediments. *Clim. Past* 12, 75–90.
- Niklewski, J., van Zeist, W., 1970. A Late Quaternary pollen diagram from north-western Syria. *Acta Bot. Neerl.* 19, 737–754.
- Ohlwein, C., Wahl, E.R., 2012. Review of probabilistic pollen-climate transfer methods. *Quat. Sci. Rev.* 31, 17–29.
- Orland, I.J., Bar-Matthews, M., Ayalon, A., Matthews, A., Kozdon, R., Ushikubo, T., Valley, J.W., 2012. Seasonal resolution of Eastern Mediterranean climate change since 34 ka from a Soreq Cave speleothem. *Geochim. Cosmochim. Acta* 89, 240–255.
- Petit, J.R., Jouzel, J., Raynaud, D., Barkov, N.I., Barnola, J.M., Basile, I., Bender, M., Chappellaz, J., Davis, M., Delaygue, G., Delmotte, M., Kotlyakov, V.M., Legrand, M., Lipenkov, V.Y., Lorius, C., Pépin, L., Ritz, C., Saltzman, E.,

- Stievenard, M., 1999. Climate and atmospheric history of the past 420,000 years from the Vostok ice core, Antarctica. *Nature* 399, 429–436.
- Pickarski, N., Kwiecien, O., Langgut, D., Litt, T., 2015. Abrupt climate and vegetation variability of eastern Anatolia during the last glacial. *Clim. Past* 11, 1491–1505.
- Prentice, I.C., Cleator, S.F., Huang, Y.H., Harrison, S.P., Roulstone, I., 2017. Reconstructing ice-age palaeoclimates: quantifying low-CO₂ effects on plants. *Glob. Planet. Chang.* 149, 166–176.
- Prentice, I.C., Guiot, J., Harrison, S.P., 1992. Mediterranean vegetation, lake levels and palaeoclimate at the Last Glacial Maximum. *Nature* 360, 658–660.
- R Core Team, 2016. R: A Language and Environment for Statistical Computing. R Foundation for Statistical Computing, Vienna, Austria. Available at: <http://www.R-project.org/>.
- Ramsey, C.B., 2009. Bayesian analysis of radiocarbon dates. *Radiocarbon* 51, 337–360.
- Rasmussen, S.O., Bigler, M., Blockley, S.P., Blunier, T., Buchardt, S.L., Clausen, H.B., Cvijanovic, I., Dahl-Jensen, D., Johnsen, S.J., Fischer, H., Gkinis, V., Guillemin, M., Hoek, W.Z., Lowe, J.J., Pedro, J.B., Popp, T., Seierstad, I.K., Steffensen, J.P., Svensson, A.M., Vallelonga, P., Vinther, B.M., Walker, M.J.C., Wheatley, J.J., Winstrup, M., 2014. A stratigraphic framework for abrupt climatic changes during the Last Glacial period based on three synchronized Greenland ice-core records: refining and extending the INTIMATE event stratigraphy. *Quat. Sci. Rev.* 106, 14–28.
- Reille, M., 1995. Pollen et spores d'Europe et d'Afrique du Nord: supplément 1. Laboratoire de Botanique Historique et Palynologie, Marseille.
- Reille, M., 1998. Pollen et spores d'Europe et d'Afrique du Nord: supplément 2. Laboratoire de Botanique Historique et Palynologie, Marseille.
- Reille, M., 1999. Pollen et spores d'Europe et d'Afrique du Nord, 2 ed. Laboratoire de Botanique Historique et Palynologie, Marseille.
- Reimer, P.J., Bard, E., Bayliss, A., Beck, J.W., Blackwell, P.G., Ramsey, C.B., Buck, C.E., Cheng, H., Edwards, R.L., Friedrich, M., Grootes, P.M., Guilderson, T.P., Haflidason, H., Hajdas, I., Hatte, C., Heaton, T.J., Hoffmann, D.L., Hogg, A.G., Hughen, K.A., Kaiser, K.F., Kromer, B., Manning, S.W., Niu, M., Reimer, R.W., Richards, D.A., Scott, E.M., Southon, J.R., Staff, R.A., Turney, C.S.M., van der Plicht, J., 2013. Intcal13 and Marine13 radiocarbon age calibration curves 0–50,000 Years cal BP. *Radiocarbon* 55, 1869–1887.
- Robinson, S.A., Black, S., Sellwood, B.W., Valdes, P.J., 2006. A review of palaeoclimates and palaeoenvironments in the Levant and Eastern Mediterranean from 25,000 to 5000 years BP: setting the environmental background for the evolution of human civilisation. *Quat. Sci. Rev.* 25, 1517–1541.
- Rohling, E.J., 2013. Quantitative assessment of glacial fluctuations in the level of Lake Lisan, Dead Sea rift. *Quat. Sci. Rev.* 70, 63–72.
- Rollefson, G.O., Köhler-Rollefson, I., 1992. Early neolithic exploitation patterns in the Levant: cultural impact on the environment. *Popul. Environ.* 13, 243–254.
- Rossignol-Strick, M., 1995. Sea-land correlation of pollen records in the eastern Mediterranean for the glacial-interglacial transition. *Quat. Sci. Rev.* 14, 893–915.
- Schiebel, V., 2013. Vegetation and Climate History of the Southern Levant during the Last 30,000 Years Based on Palynological Investigation. University of Bonn, Bonn, p. 104.
- Schiebel, V., Litt, T., 2018. Holocene vegetation history of the southern Levant based on a pollen record from Lake Kinneret (Sea of Galilee), Israel. *Veg. Hist. Archaeobotany* 27, 577–590.
- Schiller, G., Ungar, E.D., Cohen, S., Herr, N., 2010. Water use by Tabor and Kermes oaks growing in their respective habitats in the Lower Galilee region of Israel. *For. Ecol. Manag.* 259, 1018–1024.
- Schiller, G., Ungar, E.D., Cohen, Y., 2002. Estimating the water use of a sclerophyllous species under an East-Mediterranean climate: I. Response of transpiration of *Phillyrea latifolia* L. to site factors. *For. Ecol. Manag.* 170, 117–126.
- Schölzel, C., 2006. Palaeoenvironmental Transfer Functions in a Bayesian Framework with Application to Holocene Climate Variability in the Near East. University of Bonn, Bonn, p. 204.
- Schölzel, C.A., Hense, A., Hübl, P., Kühl, N., Litt, T., 2002. Digitization and geo-referencing of botanical distribution maps. *J. Biogeogr.* 29, 851–856.
- Seierstad, I.K., Abbott, P.M., Bigler, M., Blunier, T., Bourne, A.J., Brook, E., Buchardt, S.L., Buizert, C., Clausen, H.B., Cook, E., Dahl-Jensen, D., Davies, S.M., Guillemin, M., Johnsen, S.J., Pedersen, D.S., Popp, T.J., Rasmussen, S.O., Severinghaus, J.P., Svensson, A., Vinther, B.M., 2014. Consistently dated records from the Greenland GRIP, GISP2 and NGRIP ice cores for the past 104 ka reveal regional millennial-scale $\delta^{18}\text{O}$ gradients with possible Heinrich event imprint. *Quat. Sci. Rev.* 106, 29–46.
- Shea, J.J., 2008. Transitions or turnovers? Climatically-forced extinctions of Homo sapiens and Neanderthals in the East Mediterranean levant. *Quat. Sci. Rev.* 27, 2253–2270.
- Stein, M., 2001. The sedimentary and geochemical record of Neogene-Quaternary water bodies in the Dead Sea Basin – inferences for the regional paleoclimatic history. *J. Paleolimnol.* 26, 271–282.
- Stein, M., 2014. The evolution of neogene-quaternary water-bodies in the Dead Sea Rift Valley. In: Garfunkel, Z., Ben-Avraham, Z., Kagan, E. (Eds.), *Dead Sea Transform Fault System: Reviews*. Springer, Dordrecht, pp. 279–316.
- Stein, M., Ben-Avraham, Z., Goldstein, S., Agnon, A., Ariztegui, D., Brauer, A., Haug, G., Ito, E., Yasuda, Y., 2011a. Deep drilling at the Dead Sea. *Sci. Drill.* 11, 46–47.
- Stein, M., Ben-Avraham, Z., Goldstein, S.L., 2011b. Dead Sea deep cores: a window into past climate and seismicity. *Eos, Trans. Am. Geophys. Union* 92, 453.
- Stein, M., Starinsky, A., Katz, A., Goldstein, S.L., Machlus, M., Schramm, A., 1997. Strontium isotopic, chemical, and sedimentological evidence for the evolution of Lake Lisan and the Dead Sea. *Geochem. Cosmochim. Acta* 61, 3975–3992.
- Stein, M., Torfstein, A., Gavrieli, I., Yechiel, Y., 2010. Abrupt aridities and salt deposition in the post-glacial Dead Sea and their North Atlantic connection. *Quat. Sci. Rev.* 29, 567–575.
- Stockhecke, M., Timmermann, A., Kipfer, R., Haug, G.H., Kwiecien, O., Friedrich, T., Menviel, L., Litt, T., Pickarski, N., Anselmetti, F.S., 2016. Millennial to orbital-scale variations of drought intensity in the Eastern Mediterranean. *Quat. Sci. Rev.* 133, 77–95.
- Stockmar, J., 1971. Tablets with spores used in absolute pollen analysis. *Pollen Spores* 13, 615–621.
- Swain, A.M., 1973. A history of fire and vegetation in northeastern Minnesota as recorded in lake sediments. *Quat. Res.* 3, 383–396.
- Thoma, B.M., 2017. Palaeoclimate Reconstruction in the Levant and on the Balkans. University of Bonn, Bonn, p. 266.
- Torfstein, A., Goldstein, S.L., Kagan, E.J., Stein, M., 2013a. Integrated multi-site U–Th chronology of the last glacial Lake Lisan. *Geochem. Cosmochim. Acta* 104, 210–231.
- Torfstein, A., Goldstein, S.L., Kushnir, Y., Enzel, Y., Haug, G., Stein, M., 2015. Dead Sea drawdown and monsoonal impacts in the Levant during the last interglacial. *Earth Planet. Sci. Lett.* 412, 235–244.
- Torfstein, A., Goldstein, S.L., Stein, M., Enzel, Y., 2013b. Impacts of abrupt climate changes in the levant from last glacial Dead Sea levels. *Quat. Sci. Rev.* 69, 1–7.
- Turner, R., Roberts, N., Eastwood, W.J., Jenkins, E., Rosen, A., 2010. Fire, climate and the origins of agriculture: micro-charcoal records of biomass burning during the last glacial–interglacial transition in Southwest Asia. *J. Quat. Sci.* 25, 371–386.
- Tzedakis, P.C., 1994. Hierarchical biostratigraphical classification of long pollen sequences. *J. Quat. Sci.* 9, 257–259.
- Ungar, E.D., Rotenberg, E., Raz-Yaseef, N., Cohen, S., Yakir, D., Schiller, G., 2013. Transpiration and annual water balance of Aleppo pine in a semiarid region: implications for forest management. *For. Ecol. Manag.* 298, 39–51.
- Vaks, A., Bar-Matthews, M., Ayalon, A., Matthews, A., Frumkin, A., Dayan, U., Halicz, L., Almogi-Labin, A., Schilman, B., 2006. Paleoclimate and location of the border between Mediterranean climate region and the Sahara–Arabian Desert as revealed by speleothems from the northern Negev Desert, Israel. *Earth Planet. Sci. Lett.* 249, 384–399.
- Vaks, A., Bar-Matthews, M., Ayalon, A., Schilman, B., Gilmour, M., Hawkesworth, C.J., Frumkin, A., Kaufman, A., Matthews, A., 2003. Paleoclimate reconstruction based on the timing of speleothem growth and oxygen and carbon isotope composition in a cave located in the rain shadow in Israel. *Quat. Res.* 59, 182–193.
- Valladas, H., Reyss, J.L., Joron, J.L., Valladas, G., Bar-Yosef, O., Vandermeersch, B., 1988. Thermoluminescence dating of Mousterian Tro-Cro-Magnon' remains from Israel and the origin of modern man. *Nature* 331, 614–616.
- van Zeist, W., Baruch, U., Bottema, S., 2009. Holocene palaeoecology of the Hula area, northeastern Israel. In: Kaptijnand, E., Petit, L.P. (Eds.), *A timeless vale. Archaeological and related essays on the Jordan Valley in honour of Gerrit van der Kooij on the occasion of his sixty-fifth birthday*. Leiden University Press., Leiden, pp. 29–64.
- van Zeist, W., Bottema, S., 2009. A palynological study of the Acheulian site of Gesher Benot Ya'aqov, Israel. *Veg. Hist. Archaeobotany* 18, 105–121.
- van Zeist, W., Woldring, H., Stapert, D., 1975. Late Quaternary vegetation and climate of southwestern Turkey. *Palaeohistoria* 17, 55–143.
- Vannière, B., Colombaroli, D., Chapon, E., Leroux, A., Tinner, W., Magny, M., 2008. Climate versus human-driven fire regimes in Mediterranean landscapes: the Holocene record of Lago dell'Accesa (Tuscany, Italy). *Quat. Sci. Rev.* 27, 1181–1196.
- Vannière, B., Power, M.J., Roberts, N., Tinner, W., Carrión, J., Magny, M., Bartlein, P., Colombaroli, D., Daniau, A.L., Finsinger, W., Gil-Romera, G., Kaltenrieder, P., Pini, R., Sadori, L., Turner, R., Valsecchi, V., Vescovi, E., 2011. Circum-Mediterranean fire activity and climate changes during the mid-Holocene environmental transition (8500–2500 cal. BP). *Holocene* 21, 53–73.
- Waldmann, N., Stein, M., Ariztegui, D., Starinsky, A., 2009. Stratigraphy, depositional environments and level reconstruction of the last interglacial Lake Samra in the Dead Sea basin. *Quat. Res.* 72, 7–15.
- Weinstein-Evron, M., 1983. The paleoecology of the early Wurm in the Hula basin. *Israel. Paléorient* 9, 5–19.
- Weinstein-Evron, M., Vogel, J., Kronfeld, J., 2001. Further attempts at dating the palynological sequence of the Hula Lo7 core, upper Jordan Valley, Israel. *Radiocarbon* 43, 561–570.
- Whitlock, C., Higuera, P.E., McWethy, D.B., Briles, C.E., 2010. Paleoecological perspectives on fire ecology: revisiting the fire-regime concept. *Open Ecol. J.* 3, 6–23.
- Whitlock, C., Larsen, C., 2001. Charcoal as a fire proxy. In: Smol, J.P., Birks, H.J.B., Last, W.M., Bradley, R.S., Alverson, K. (Eds.), *Tracking Environmental Change Using Lake Sediments. Volume 3: Terrestrial, Algal, and Siliceous Indicators*. Kluwer Academic Publishers, Dordrecht, pp. 75–97.
- Yasuda, Y., Kitagawa, H., Nakagawa, T., 2000. The earliest record of major anthropogenic deforestation in the Ghab Valley, northwest Syria: a palynological study. *Quat. Int.* 73 (74), 127–136.
- Zaarur, S., Affek, H.P., Stein, M., 2016. Last glacial-Holocene temperatures and

- hydrology of the Sea of Galilee and Hula Valley from clumped isotopes in Melanopsis shells. *Geochem. Cosmochim. Acta* 179, 142–155.
- Zhao, Y., Liu, H., Li, F., Huang, X., Sun, J., Zhao, W., Herzschuh, U., Tang, Y., 2012. Application and limitations of the Artemisia/Chenopodiaceae pollen ratio in arid and semi-arid China. *Holocene* 22, 1385–1392.
- Zohary, M., 1962. *Plant Life of Palestine: Israel and Jordan*. The Ronald Press Company, New York.
- Zohary, M., 1982. *Vegetation of Israel and Adjacent Areas*. Dr. Ludwig Reichert, Wiesbaden.